UNIVERSIDAD NACIONAL AUTÓNOMA DE MÉXICO
PROGRAMA DE MAESTRÍA Y DOCTORADO EN INGENIERÍA
INGENIERÍA ELÉCTRICA-CONTROL

SECOND ORDER ROBUST EXACT DIFFERENTIATOR GAIN DESIGN: A FREQUENCY DOMAIN APPROACH

TESIS

QUE PARA OPTAR POR EL GRADO DE
MAESTRO EN INGENIERÍA

PRESENTA
JONATHAN ESCOBAR HERNÁNDEZ

TUTOR PRINCIPAL
DR. LEONID FRIDMAN, FACULTAD DE INGENIERÍA UNAM

CIUDAD UNIVERSITARIA, CDMX, JUNIO 2022

JURADO ASIGNADO:

Presidente:	Dra. María Cristina Verde Rodarte
Secretario:	Dr. Marco Antonio Arteaga Pérez
$1^{er.}$ Vocal:	Dr. Leonid Fridman
$2^{do.}$ Vocal:	Dr. Jaime Alberto Moreno Pérez
$3^{er.}$ Vocal:	Dr. Jorge Ángel Dávila Montoya

Lugar donde se realizó la tesis: Posgrado de Ingeniería, Ciudad Universitaria

TUTOR DE TESIS:

DR. LEONID FRIDMAN

FIRMA

Agradecimientos

A mi madre María Victoria y a mi padre Juan Jorge por su inmenso cariño y su apoyo durante toda mi vida y en particular durante esta etapa. Me debo a ustedes y a ustedes siempre estaré agradecido.

Al Dr. Leonid Fridman por la oportunidad de conocer un poco más de cerca el ámbito de investigación en el área de control por modos deslizantes; por su amable y paciente guía durante la realización de este trabajo y por todas las atenciones procuradas a mi y a todos sus estudiantes.

Al Dr. Jaime Moreno y a todos los asistentes al seminario de modos deslizantes por la discusión académica semana a semana y por sus comentarios acerca del trabajo; en particular a Jesús y Ulises por su orientación y buena disposición para conmigo.

A los integrantes del jurado por su realimentación; en particular a la Dra. Cristina Verde por la asertividad de sus observaciones.

A los profesores del colegio de control por las enseñanzas recibidas y por la entereza con la que emprendieron sus labores docentes ante la emergente contingencia sanitaria.

A mis colegas de generación por el buen compañerismo durante el posgrado.

A la Universidad Nacional Autónoma de México por la oportunidad de continuar mi formación académica.

Abstract

Via a frequency approach, the issue of the design of gains for the second order robust exact differentiator introduced by Levant is studied under the presence of a delay. Assuming that the resultant high-frequency oscillatory motion due to the introduced nonideality could be decomposed in its fast and slow components, a describing function is computed for the differentiator. By using such describing function a selection criterion for the differentiator gains ensuring orbital stability and a local minimization of the oscillations amplitude along the estimate of the first derivative is found. According to the proposed criterion, some sets of gains are determined. Furthermore, for the ideal case without delay, the feasibility of those gains sets is shown by proving that the differentiator preserves its stability properties under such parameters settings; moreover, an extension of the results to a case with more relaxed assumptions on the input signal is also suggested. Finally, simulations are performed in order to show the consistency of the results under the stated assumptions illustrating the performance of one of the computed gains sets.

Contents

List of Figures

List of Tables

Acronyms

n-RED n-th order robust exact differentiator.

2-RED second order robust exact differentiator.

AF associated form.

CTA continuous twisting algorithm.

DF describing function.

DI differential inclusion.

DIDF dual-input describing function.

GF generalized form.

HB harmonic balance.

HOSM high order sliding mode.

LF Lyapunov function.

LMI linear matrix inequality.

LPRS locus of a perturbed relay system.

ODE ordinary differential equation.

OF output feedback.

PD positive definite.

PID-CSMC PID-like continuous sliding mode controller.

RED robust exact differentiator.

SMC sliding mode control.

SOS sum of squares.

STA super twisting algorithm.

STC super twisting controller.

URED uniform robust exact differentiator.

VSC variable structure control.

Chapter 1

Introduction

1.1 State of the Art

Real-time differentiation is an important issue concerning the fields of control theory and applications. Closely related to the task of state observation, differentiators turn to be particularly useful to estimate the derivatives of a given signal, when no further measurements are available; Besides estimation and identification, another important application of differentiators lies in the design and implementation of output feedback (OF) control schemes.

One of the main difficulties related to the task of on-line differentiation in real systems is the ubiquitous presence of measurement noise along the base signal; since the differentiation of such small high-frequency components may lead to large derivatives, the resultant estimation might be greatly deteriorated. A classical approach to deal with this problem consists in the construction of linear differentiators along with the use of low-pass filters to damp the noise; the main of such methods relies on approximating the transfer function of an ideal differentiator on a fixed frequency band (Rabiner & Steiglitz, 1970). Moreover, stochastic features of the noise may also be considered in order to estimate the derivatives of the base signal (Kalman, 1960).

Some other well known linear techniques which might be applied in a real-time environment rely on observer-based or algebraic approaches such as the high-gain observers (Dabroom & Khalil, 1997) and algebraic differentiators (Mboup et al., 2009), respectively; additionally, some observer-based approaches have exploited the homogeneity property to develop nonlinear continuous differentiation algorithms (Andrieu et al., 2008; Perruquetti et al., 2008).

Besides the aforementioned approaches, the robust exact differentiator (RED) (Levant, 1998; Levant, 2003) has become a very popular tool to tackle the real-time differentation problem. Based on sliding-modes techniques, this differentiator provides a convenient method to estimate the derivative of a noisy signal. In the absence of noise, the n-th order robust exact differentiator (n-RED) achieves exact convergence to the n derivatives of the input signal, when its $n+1$-th derivative remains uniformly bounded by a known constant. Furthermore, it does so in finite time as has been shown both using geometric methods (Levant, 1998) and homogeneity properties (Levant, 2003). Regarding the nonideal case, the attainable precision of the n-RED due to the effects of measurement noise and discrete-time sampling can be assessed as a function of the noise magnitude upper bound and the sampling step, respectively (Levant, 2003).

Since the introduction of the RED in the late 1990s, research has been fostered aiming at the en-

hancement of the performance of this differentation algorithm, leading to developments such as the uniform robust exact differentiator (URED) (Cruz-Zavala et al., 2011), whose convergence time is independent of the initial conditions of the differentiation error, or the robust exact filtering differentiator (Levant & Livne, 2020) that is capable of filtering out unbounded noises with small average values while preserving the features of the standard RED. Regarding its computer-based application to real-time systems, some discretization schemes aiming to render discrete-time versions of this kind of differentiatiors while preserving the accuracy of their continuous-time counterparts have been introduced during the last decade (Livne & Levant, 2014; Barbot et al., 2020).

Despite all this advance, the RED as introduced by Levant in 2003 remains a simple and effective solution to the differentiation problem given a properly designed set of gains; for this reason, the main problem concerning the use of this differentiation algorithm relies in the appropriate selection of such parameters. As first introducing this differentiator, Levant (2003) stated that the best way to choose its parameters was by computer simulation, hence reporting a set of suitable gains for the fifth-order version from which the gains for the low-order differentiators could be selected in a straightforward way. This set of parameters has been frequently used due to the homogeneity properties of the differentiatior which allows to scale them according to each case requirements. Elaborating on the gain selection issue, Reichhartinger and Spurgeon (2018) remarked that although the parameters of the first order robust exact differentiator (RED) may be selected based on the available theoretical convergence conditions for the case of reconstructing the first derivative, the parameters setting for the case of high-order differentiators may turn into a more difficult task and it could be complicated to achieve a good performance over a broad domain of application from a single set of gains.

In the abscence of noise and $f(t)$, $t \geq 0$ denoting the signal to be differentiated, the only assumption required by the first order RED is that the first derivative of $f(t)$ has a known finite Lipszchitz constant $\mathcal{L}$ Levant (1998), that is, that the input signal belongs to the class of signals with bounded second derivative

$$\left|\ddot{f}(t)\right| \leq \mathcal{L}. \tag{1.1}$$

For the n-RED, the assumption on the input signal follows in a similar way. Moreover, the same requirement holds for a noisy signal, where the Lipschitz condition is to be considered on the derivative of the base signal. Therefore, a bound $\mathcal{L}$ has to be known beforehand in order to select the differentiator parameters accordingly. Further research has led to results aiming to simplify the task of case-based gains tuning, allowing a broader class of input signals to be considered. For example, in the work by Moreno (2018) an exact differentiation with varying gains was proved for signals whose derivatives are bounded by a known time-varying function, that is, accounting for a varying $\mathcal{L}(t)$ instead of a constant $\mathcal{L}$. Also in 2018, Reichhartinger and Spurgeon proposed a design paradigm with adaptive gains based on a pseudo-linear representation of the system; likewise, Obeid et al. (2018) developed an adaptation algorithm for the gains of the RED based on barrier function.

Aside from the aformentioned results involving time-varying or adaptive schemes, there exist some tuning procedures for the standard case with constant gains, particularly for the first order RED which shares some of the parameter selection criteria with the super twisting algorithm (STA) (Levant, 1998; Shtessel et al., 2014). The tuning for second and higher differentiation orders has been less studied, though. However, the introduction of a Lyapunov function (LF) for the second order robust exact differentiator (2-RED) (Moreno, 2012) brought new insights to such study, enabling to inquiry into properties like convergence time and robustness that were hardly

approached under the back then existent geometric and homogeneity paradigms; further results followed thereafter. Trying to circumvent the cumbersome task of dealing with the numerous inequalities arisen from the design methodology based on a generalization of Young inequalities in Moreno (2012), Ortiz-Ricardez et al. (2015) devised a new LF for the 2-RED by using a generalized-forms approach which besides being continuous, was also differentiable. Furthermore, in 2018, Sanchez, Cruz-Zavala, et al. generalized such design approach relying on a sum-of-squares method for both the cases of continuous and discontinuous differentiators, comprising the n-RED as a particular instance. Similarly, an account of a family of smooth LFs for the n-RED was presented in Cruz-Zavala and Moreno (2018), allowing to study the convergence and performance properties as well as consider the design of gains for such differentiators. More recently, elaborating on the work by Cruz-Zavala and Moreno (2018), Merino (2019) introduced a methodology that, exploiting the recursive structure of the RED, enables to design the gains of a higher-order differentiator based on a given set of gains for a lower-order one.

As a sliding-modes algorithm, the RED is no excluded from the so-called *chattering* phenomenon, that is, high-frequency oscillations which arise due to the imposibility of attaining the theoretically infinite switching frequency demanded by such algorithms in a real environment (see Levant, 2010, for a formal account on *chattering*). This, generally undesirable, phenomenon is the main drawback that has hindered the broader application of these techniques due to the potentially harmful effects to actuators which may arise in a control system. Therefore, great part of the research on sliding mode control (SMC) has been aimed at the study of *chattering* and its mitigation (Utkin & Lee, 2006), motivating advancements such as the development of the so-called continuous high order sliding modes (HOSMs) (Fridman et al., 2015).

Regarding the *chattering* analysis, the use of frequency methods constitutes a direction within the sliding-modes research which seeks to tackle problems related to the existence and parameters determination of periodic motions, the stability of limit cycles and the input-output problem (Boiko, 2005). Accordingly, the main approaches which have been explored since their application to relay-feedback systems comprise methods such as the describing function (DF) (Atherton, 1975, as cited in Boiko, 2005), the Tsypkin's one (Tsypkin, 1984, as cited in Boiko, 2005) and the locus of a perturbed relay system (LPRS) (Boiko, 2003). Although being only capable to yield approximate results, providing less accuracy in comparison with the other two referred techniques, the DF method has allowed to develop systematic approaches to analyze *chattering* (Boiko et al., 2007); it has also been proven to be a convenient method to study various continuous and discontinuous SMC algorithms under a unified approach, allowing to draw a performance comparison among them (Pérez-Ventura & Fridman, 2019b). Furthermore, it has been succesfully applied to aid the gain design of some sliding-mode controllers such as the super twisting controller (STC) (Pérez-Ventura & Fridman, 2019a) and the PID-like continuous sliding mode controller (PID-CSMC) (Pérez-Ventura et al., 2021), enabling to develop a methodology to find suboptimal gains sets which allow to reduce either the *chattering* amplitude or the average power required to maintain the system's trajectories into a real sliding motion.

With respect to the study of the RED via frequency methods, an antecedent can be found in Boiko et al. (2008), where the transfer properties of a STA-based differentiator due to a external input were investigated by introducing the equivalent gain concept. However, neither the case of the second-order differentiator nor the parameters design were considered in such work. Therefore, a DF-based approach such as the aforementioned one may be explored to tackle the issue of the design of gains for the 2-RED in order to yield criteria for the parameter selection aiming to reduce the *chattering* amplitude of the first derivative estimate and, consequently, improve the performance

during the differentiation task.

1.2 Motivation

Although the first derivative of a given signal can already be estimated by using a first order RED, as remarked by Levant (2003), for every $l < k$, a k-th order differentiator allows for a much better accuracy of the l-th derivative than an l-th order differentiator. Due to this fact, it is more convenient to work with a 2-RED instead of its first order counterpart when just the first derivative is required. Moreover, concerning the design of OF control schemes, the use of 2-RED-based observers has been proven to result more advantageous in comparison with its first-order counterpart. For example, for the STC, Chalanga et al. (2016) showed that the stabilization of a perturbed double integrator cannot be achieved by using a STA-based observer in the OF control scheme, that is, by using a first order RED. They proved that for the resultant control law an additional term is required in order to attain the desired second-order sliding mode along a relative degree 1 sliding surface, leading to a discontinuous control signal, though. On the contrary, if a higher-order observer based on the 2-RED is considered in the OF control scheme, the stabilization is accomplished not only by means of a continuous control signal, but also allowing an improved precision on the sliding manifold. Another result which points in favor of the use of the 2-RED can be found in Sanchez, Moreno, and Fridman (2018), regarding the continuous twisting algorithm (CTA). By studying two OF control schemes, one based on the first order RED and the other based on the 2-RED, they showed that whereas in the case of the lower-order RED homogeneity is lost, by using the higher-order one it can be retained, preserving the robustness and accuracy properties of the state feedback CTA. Moreover, they pointed out the establishment of a separation principle in the OF design considering the 2-RED, allowing to design the controller and the observer indepently from each other.

From this perspective, despite the additional tuning parameter, the 2-RED may turn to be a better option in cases such as the mentioned ones; on account of that, some gain selection criteria which allows for a better performance of the differentiator and consequently of the whole OF control scheme would be a valuable design tool.

1.3 Problem Statement

Consider the 2-RED (Levant, 2003) in its so-called nonrecursive form:

$$\begin{aligned} \dot{z}_0 &= -k_0 \left| z_0 - f(t) \right|^{\frac{2}{3}} \operatorname{sign}(z_0 - f(t)) + z_1, \\ \dot{z}_1 &= -k_1 \left| z_0 - f(t) \right|^{\frac{1}{3}} \operatorname{sign}(z_0 - f(t)) + z_2, \\ \dot{z}_2 &= -k_2 \operatorname{sign}(z_0 - f(t)), \end{aligned} \tag{1.2}$$

where $f(t), t > 0$ is a function whose third derivative has a known upperbound, that is, $\left| f^{(3)}(t) \right| \leq L$. For the ideal continuous-time case in absence of noise, the following equalities are established after a finite time:

$$z_0 = f(t), \quad z_1 = \dot{f}(t), \quad z_2 = \ddot{f}(t)$$

Nevertheless, from a practical point of view, its real discrete-time application may give rise to the *chattering* phenomenon, causing the trajectories z_i to exhibit high frequency oscillations in a neighborhood of the base signals $f^{(i)}(t)$, $i = 0, 1, 2$. Accounting for the nonidealities which may lead to this behavior during the measurement or processing tasks, a scalar constant delay is introduced in order to study the differentiator via the closed loop scheme shown in Fig. 1.1; furthermore, the zero function $f(t) = 0$ is considered at the input in order to study the steady-state oscillatory response via the single-sinusoid DF approach. Therefore, under such assumption, the problem lies in finding some guidelines for the selection of gains which ensure a local minimum achievable amplitude of the *chattering* induced by the introduction of the time delay, in accord with the methodology exposed by Pérez-Ventura et al. (2021). It is important to remark that the goal is not to achieve a global minimum amplitude, but to ensure that given a pair of gains, the third one completing the set allows to yield the attainable minimum *chattering* for such pair. In some works on the gain design for SMC algorithms (Pérez-Ventura & Fridman, 2019a; Pérez-Ventura et al., 2021), the paremeter tuning which yields such local minimum by the selection of one of the gains while fixing the rest of them has been referred to as *suboptimal*. Accordingly, the gain sets computed via the guidelines proposed in this work may be referred as *suboptimal* too.

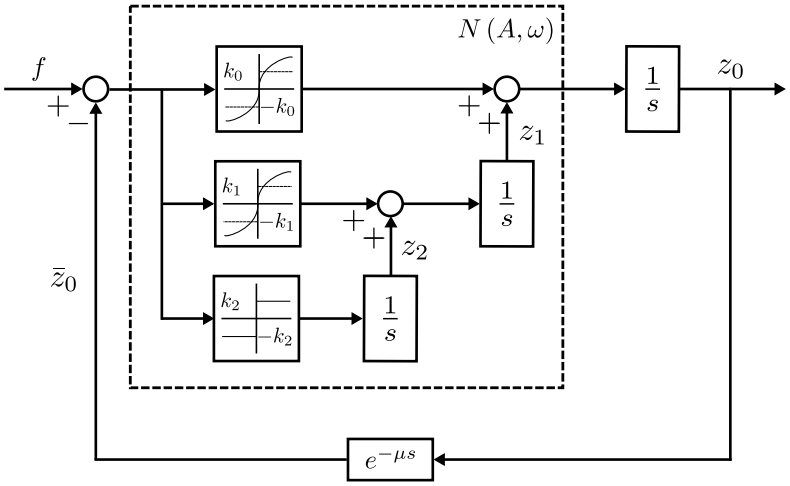

Figure 1.1: Robust exact differentiator diagram.

1.4 Objectives

The main objectives of this work, which also correspond to its contributions, are the following:

1. to compute, as a function of the 2-RED gains, the approximated values for the amplitude of possible oscillations arisen by the presence of a time delay,
2. to find a criterion for the selection of the differentiator gains which ensure a local minimization of the calculated oscillations amplitude,
3. to show that if the above-mentioned oscillations exist, they are orbitally asymptotically stable,
4. to prove for the ideal case without delay that the differentiator keeps global finite time convergence for some of the parameter sets found via the proposed criterion.

1.5 Outline

After having provided an introduction to the present work in the current chapter, in Chapter 2, the case study of this work, that is, the 2-RED, is presented. Moreover, a brief overview of SMC and the *chattering* phenomenon is given as well as some useful preliminaries.

In Chapter 3, the considered methodology for suboptimal gains design is introduced and some of such sets is determined; additionally, simulation examples are provided to depict the achievable steady-state performance of one of those parameters sets.

In Chapter 4, Lyapunov stability is studied for both the nominal and perturbed cases of the 2-RED error dynamics for the given suboptimal gains sets.

Finally, in Chapter 5, some concluding remarks are stated.

Remark on Notation

Let $\lceil\cdot\rfloor^{\rho} = |\cdot|^{\rho}\operatorname{sign}(\cdot)$ denote the so-called signed power function for any $\rho \in \mathbb{R}_{\geq 0}$ such that $\mathbb{R}_{\geq 0}$ denotes the nonnegative reals. The same notation holds likewise for the sets of nonnegative rationals $\mathbb{Q}_{\geq 0}$ and nonnegative integers $\mathbb{Z}_{\geq 0}$.

Chapter 2

Preliminaries

2.1 Sliding Modes

Sliding mode control (SMC) is one of the main robust control approaches for dealing with uncertain systems. It is a particular type of the variable structure control (VSC) techniques that involve a set of feedback control laws and a decision rule, called switching function, that allows to switch among the controllers, leading to different subsystems with fixed control structures valid for specific regions of the system state space, hence its name (Emelyanov et. al., 1970, as cited in Hung et al., 1993). As such, SMC relies on the deliberate change of the control law based on some defined state-dependent rules in order to drive the trajectories to a constrained region of the state space where a desired behavior is attained.

2.1.1 Chattering Phenomenon

According to the SMC jargon, the region of the state space where a determined constraint is kept is referred to as the sliding surface. Thus, denoting such constraint as $\varsigma(x) = 0$, with x being the system state, ς is the so-called sliding variable that acts as the decision rule to switch the control law. This terminology is due to the two stages which can be distinguished in the trajectories of a system under the action of a SMC algorithm; namely, the reaching phase in which the trajectories are driven towards the sliding surface, and the sliding phase in which they remain within a neighbourhood of such surface *sliding* along it as depicted in Fig. 2.1.

A system whose dynamics are subject to the constraint kept during the sliding phase is said to be in sliding motion or to have attained a sliding mode; moreover, if the trajectories remain constrained to lie exactly over the sliding surface, then such behavior is referred to as an ideal sliding mode. Nevertheless, such an ideal behavior only exists theoretically for time-continuous systems without delays due to the fact that it would imply a control signal commuting at an infinite frequency on account of the discontinuities usually found in the driving control laws. Therefore, in real systems, the presence of switching imperfections owing to time delays, and nonmodeled dynamics in both sensors and actuators prevent attaining an ideal sliding motion, giving rise to a dynamic behavior consisting on high-frequency oscillations across the vicinity of the sliding surface (Emelyanov, 1963, as cited in Fossard & Floquet, 2002). Since this phenomenon known as *chattering* can be detrimental to both plant and actuators, research has been encouraged towards developing techniques to diminish it in order to advance the application of this control methodology. This has led to the

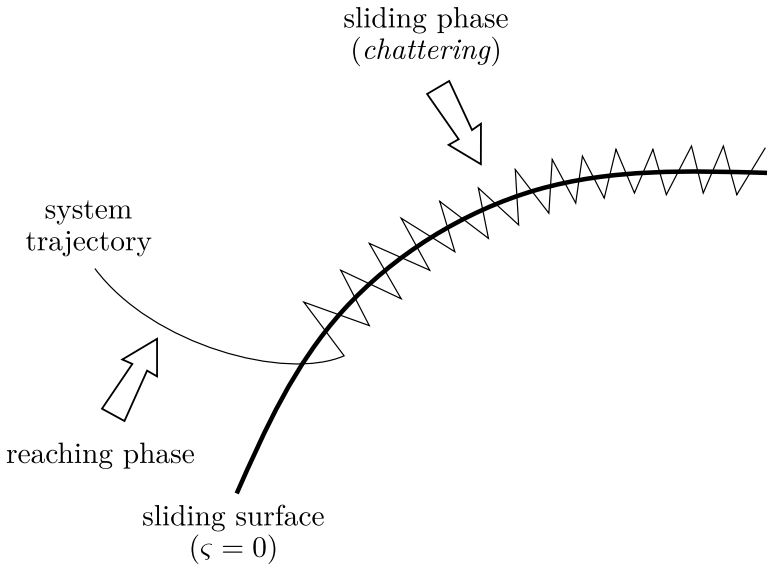

Figure 2.1: Sliding motion and the *chattering* phenomenon.

development of numerous SMC algorithms which can be grouped in the so-called sliding modes generations depending on some of its features (Fridman et al., 2015; Utkin et al., 2020).

2.2 Homogeneity

Homogeneity is the property through which some mathematical objects such as functions or vector fields scale in a consistent manner with respect to a scaling operation known as dilation (Bernuau et al., 2014). Although the concept has been refined since the first studies on homogeneous polynomials by Euler, leading to several notions of homogeneity, the definition used in this work corresponds to that of weighted homogeneity (Hermes, 1991).

2.2.1 Weighted Homogeneity

Following the notation introduced by Bernuau et al. (2014), let $x \in \mathbb{R}^n$, $\lambda \in \mathbb{R}$ and $r \in \mathbb{R}^n$, such that $r = \begin{bmatrix} r_1 & \dots & r_n \end{bmatrix}^\top$ is the so-called generalized vector of weights with $r_i > 0$. Now define the dilation operator Λ_r as

$$\begin{aligned} \Lambda_r : \mathbb{R}_{>0} \times \mathbb{R}^n &\to \mathbb{R}^n \\ (\lambda, x) &\mapsto \operatorname{diag}(\lambda^{r_1}, \dots, \lambda^{r_n})x, \end{aligned}$$

and for simplicity denote $\Lambda_r x := \Lambda_r(\lambda, x) = \operatorname{diag}(\lambda^{r_1}, \dots, \lambda^{r_n})x$, then

- a function $V : \mathbb{R}^n \to \mathbb{R}$ is said to be r-homogeneous with degree $m \in \mathbb{R}$ if for all $x \in \mathbb{R}^n$ and all $\lambda > 0$,
$$\lambda^{-m} V(\Lambda_r x) = V(x),$$

- a vector field $f : \mathbb{R}^n \to \mathbb{R}^n$ is said to be r-homogeneous with degree $m \in \mathbb{R}$ if for all $x \in \mathbb{R}^n$ and all $\lambda > 0$,
$$\lambda^{-m} \Lambda_r^{-1} f(\Lambda_r x) = f(x),$$

- a system $\dot{x} = f(x)$ is r-homogeneous if f is so.

2.2.2 Homogeneity and Differential Inclusions

The homogeneity definition can be further extended to the case of differential inclusions (DIs), such as those arising from the application of the regularization procedure due to Filippov (1988) to ordinary differential equations (ODEs) with discontinuous right-hand side; such kind of ODEs are frequently found when dealing with VSC systems. According to such procedure, an ODE with discontinuous right-hand side of the form

$$\dot{x} = f(x), \tag{2.1}$$

where f is measurable and locally essentially bounded, can be replaced with a DI defined by a set-valued map of the form

$$\dot{x} \in F(x). \tag{2.2}$$

Therefore, a solution to the ODE (2.1) is said to be understood in the sense of Filippov if it is defined as a solution to the DI (2.2).

Accordingly,

- a set-valued map $F : \mathbb{R}^n \rightrightarrows \mathbb{R}^n$ is r-homogeneous with degree $m \in \mathbb{R}$ if for all $x \in \mathbb{R}^n$ and for all $\lambda > 0$,
$$\lambda^{-m} \Lambda_r^{-1} F(\Lambda_r x) = F(x),$$
- a system $\dot{x} \in F(x)$ is homogeneous if F is so.

Moreover, if the set-valued map comes from the Filippov regularization procedure, the homogeneity property is preserved. Thus, if a vector field f is r-homogeneous of degree m, then the associated set-valued map F is r-homogeneous of degree m too (Bernuau et al., 2013).

2.3 Robust Exact Differentiation

Besides control, sliding modes find one of its main applications in the field of robust finite-time exact observation and differentiation. Regarding the differentation problem, it can be stated as follows: let $f : \mathbb{R} \to \mathbb{R}$ be the input signal given by $f(t) = f_0(t) + \xi(t)$, that is, the sum of an unknown base signal f_0 and a bounded Lebesgue-measurable noise component ξ. In addition, assume that the base function $f_0(t)$ is n-times differentiable and its n-th derivative has a Lipschitz constant $\mathcal{L} > 0$. Then, the problem consists in finding real-time robust estimation of the derivatives $f_0'(t), \ldots, f_0^{(n)}(t)$; moreover, to do so exactly in the absence of measurement noise.

2.3.1 Arbitrary Order Robust Exact Differentiator

The differentiation problem can be tackled with the n-RED (Levant, 2003)

$$
\begin{aligned}
\dot{z}_0 &= v_0, \\
v_0 &= -k_0 \lceil z_0 - f(t) \rfloor^{\frac{n}{n+1}} + z_1, \\
\dot{z}_1 &= v_1, \\
v_1 &= -k_1 \lceil z_1 - v_0 \rfloor^{\frac{n-1}{n}} + z_2, \\
&\vdots \\
\dot{z}_{n-1} &= v_{n-1}, \\
v_{n-1} &= -k_{n-1} \lceil z_{n-1} - v_{n-2} \rfloor^{\frac{1}{2}} + z_n, \\
\dot{z}_n &= -k_n \lceil z_n - v_{n-1} \rfloor^0,
\end{aligned}
\tag{2.3}
$$

where $k_i \in \mathbb{R}_{>0}, i = 0, \ldots, n$ are the differentiator gains or parameters. By exploiting the properties of the so-called signed power function $\lceil \cdot \rfloor$, the differentiator (2.3) can be also expressed in the commonly named nonrecursive form (Shtessel et al., 2014) as

$$
\begin{aligned}
\dot{z}_0 &= -k_0 \lceil z_0 - f(t) \rfloor^{\frac{n}{n+1}} + z_1, \\
\dot{z}_i &= -k_i \lceil z_0 - f(t) \rfloor^{\frac{n-i}{n+1}} + z_{i+1}, \\
&\vdots \\
\dot{z}_n &= -k_n \lceil z_0 - f(t) \rfloor.
\end{aligned}
\tag{2.4}
$$

Some of the main features of the n-RED can be stated in the following theorems.

Theorem 2.3.1 (Levant, 2003) *Given properly chosen parameters, the following equalities are established in the absence of input noises after a finite time*

$$
z_i = f_0^{(i)}(t), \quad i = 0, \ldots, n.
$$

Therefore, in absence of noise, and given a proper selection of gains, the RED states converge theoretically exactly to the sought derivatives in finite time. Regarding the nonideal case in which input noise satisfying the aforementioned assumptions is considered, the next result holds.

Theorem 2.3.2 (Levant, 2003) *Let the input noise satisfy the inequality $|f(t) - f_0(t)| \leq \epsilon$. Then the following inequalities are established in finite time for some positive constants κ_i depending exclusively on the parameters of the differentiator*

$$
\left| z_i - f_0^{(i)}(t) \right| \leq \kappa_i \epsilon^{\frac{n-i+1}{n+1}}, \quad i = 0, \ldots, n.
$$

The previous inequalities provide some means to estimate the magnitude order of the differentiator error given a known upper bound of the input noise. Finally, considering a sampling step τ, a similar result is obtained for the discrete-time case when $z_0(tj) - f(t_j)$ is substituted for $z_0 - f(t)$ with $t_j \leq t < t_{j+1}$ such that $t_{j+1} - t_j = \tau > 0$.

Theorem 2.3.3 (Levant, 2003) *Let $\tau > 0$ be the constant input sampling interval in the absence of noises. Then the following inequalities are established in finite time for some positive constants ν_i depending exclusively on the parameters of the differentiator*

$$
\left| z_i - f_0^{(0)}(t) \right| \leq \nu_i \tau^{n-i+1}, \quad i = 0, \ldots, n.
$$

2.3.2 Second Order Robust Exact Differentiator

For $n = 2$, the 2-RED is obtained from (2.4) as

$$\begin{aligned}\dot{z}_0 &= -k_0\lceil z_0 - f(t)\rfloor^{\frac{2}{3}} + z_1,\\ \dot{z}_1 &= -k_1\lceil z_0 - f(t)\rfloor^{\frac{1}{3}} + z_2,\\ \dot{z}_2 &= -k_2\lceil z_0 - ft()\rfloor^{0},\end{aligned} \tag{2.5}$$

and defining the differentiation error as $\varepsilon_i = z_i - f_0^{(i)}(t)$, the dynamics of (2.5) can be restated as

$$\begin{aligned}\dot{\varepsilon}_0 &= -k_0\lceil \varepsilon_0\rfloor^{\frac{2}{3}} + \varepsilon_1,\\ \dot{\varepsilon}_1 &= -k_1\lceil \varepsilon_0\rfloor^{\frac{1}{3}} + \varepsilon_2,\\ \dot{\varepsilon}_2 &= -k_2\lceil \varepsilon_0\rfloor^{0} + \psi(t),\end{aligned} \tag{2.6}$$

where $\psi(t) = -f_0^{(3)}(t)$. It can be easily verified that the system (2.6) is homogeneous of degree -1 with homogeneity weights $r = \begin{bmatrix}3 & 2 & 1\end{bmatrix}^\top$.

2.4 Frequency Domain Analysis Techniques

The frequency response method is one of the main tools for the analysis and design of linear systems based on the description of such systems by a complex-valued function. Although it is not possible to directly apply this method to nonlinear systems, it is possible to study a broad range of them with some analytical techniques under a frequency approach. One of such techniques is the DF method which finds its main application in the prediction and characterization of limit cycles.

2.4.1 Describing Function

This technique could be considered as an extended version of the frequency response method which allows to analyze nonlinear behavior. It basically consists on the use of quasi-linear functions to approximate the transfer characteristics of nonlinear elements; such functions are known as the DFs of the nonlinearities. Even though this method can only yield approximate results, it is a useful tool to study the effects of a large class of common nonlinearities frequently found in control systems such as saturation, dead-zone, backlash and hysteresis, among others (Atherton, 1996).

In its simplest formulation, a DF can be used to study systems which allow themselves to be accurately modeled as shown in the diagram of Fig. 2.2, that is, as a feedback loop comprising an interconnection between clearly distinguishable linear and nonlinear elements subject to no external inputs; thus, $r(t) = 0$. This technique relies on assuming beforehand the signal form at the nonlinearity input, and since this method is mainly used to study the existence and characterization of limit cycles, a sinusoid is usualy considered as the result of the filtering effect of the linear block in the loop. This assumption of low-pass properties in the linear part, which allows the driving sinusoid at the nonlinearity input to be approximated by its fundamental component, is known as the filtering hypothesis. Therefore, the major limitation of this technique is the requirement that the actual signal at the input of the nonlinear block is well approximated by that considered in the derivation of the DF (Gelb & Vander Velde, 1968).

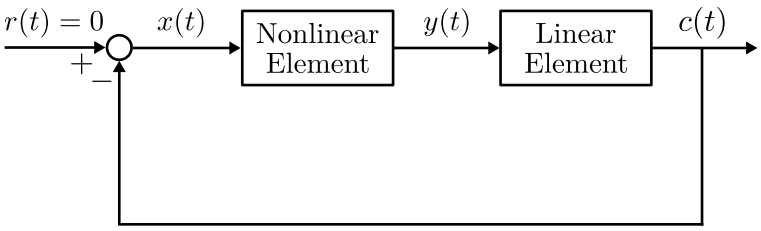

Figure 2.2: Nonlinear system.

A brief description of the formulation of a DF in its basic version, that is, for the case of an odd, static, single-valued nonlinearity, based on the exposition by Slotine and Li (1991) is outlined here.

Consider the diagram in Fig. 2.2 and assume an input

$$x(t) = A\sin(\omega t). \tag{2.7}$$

Regarding the output, it can be expressed in terms of its trigonometric Fourier series as

$$y(t) = a_0 + \sum_{n=1}^{\infty} \left[a_n \cos(n\omega t) + b_n \sin(n\omega t)\right] \tag{2.8}$$

with

$$\begin{aligned} a_0 &= \frac{1}{2\pi}\int_0^{2\pi} y(\omega t)\mathrm{d}\omega t, \\ a_n &= \frac{1}{\pi}\int_0^{2\pi} y(\omega t)\cos(n\omega t)\mathrm{d}\omega t, \\ b_n &= \frac{1}{\pi}\int_0^{2\pi} y(\omega t)\sin(n\omega t)\mathrm{d}\omega t. \end{aligned} \tag{2.9}$$

Since the considered nonlinearity is odd, $a_0 = 0$. Therefore, due to the filtering hypothesis, $y(t)$ can be approximated by its first harmonic as

$$y(t) \approx y_1(t) = a_1\cos(\omega t) + b_1\sin(\omega t) = M\sin(\omega t + \phi) \tag{2.10}$$

where

$$M(A,\omega) = \left(a_1^2 + b_1^2\right)^{\frac{1}{2}} \quad \text{and} \quad \phi(A,\omega) = \arctan\left(\frac{a_1}{b_1}\right).$$

Since the DF of a nonlinearity is defined as the complex ratio of the fundamental component of its output to its input sinusoid, and due to Euler's formula and the expression of the Fourier series in its amplitude-phase form, it can be stated as

$$N(A,\omega) = \frac{Me^{j(\omega t+\phi)}}{Ae^{j\omega t}} = \frac{M}{A}e^{j\phi} = \frac{1}{A}(b_1 + ja_1) \tag{2.11}$$

which in turn can be expressed as

$$N(A,\omega) = \frac{j}{\pi A}\int_0^{2\pi} y(\omega t)e^{-j\omega t}\mathrm{d}\omega t. \tag{2.12}$$

Moreover, for single-valued nonlinearities , $a_1 = 0$, so

$$N(A,\omega) = \frac{1}{\pi A}\int_0^{2\pi} y(\omega t)\sin(\omega t)\mathrm{d}\omega t. \tag{2.13}$$

As a result, once the DF has been computed with (2.13), it can be substituted for the nonlinearity to render an approximation of the original system and study its behavior.

2.4.2 Harmonic Balance Equation

The main application of the DF method consists in the study of steady-state oscillations such as limit cycles in nonlinear systems; this can be done as follows. Consider the diagram in Fig. 2.3, in which the DF has been substituted for the nonlinear element and the linear element is characterized by its frequency response function, assuming the existence of a self-sustained oscillation of amplitude A and frequency ω.

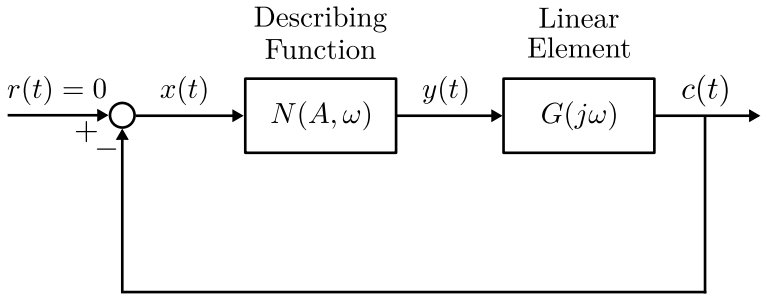

Figure 2.3: Nonlinear system with a DF substituted for the nonlinearity.

Since the input is considered to be zero, the following loop relations must hold:

$$\begin{aligned} X(j\omega) &= -G(j\omega)Y(j\omega), \\ Y(j\omega) &= N(A,\omega)X(j\omega), \end{aligned} \tag{2.14}$$

which can be expressed in matrix notation as

$$\begin{bmatrix} N(A,\omega) & -1 \\ 1 & G(j\omega) \end{bmatrix}\begin{bmatrix} X(j\omega) \\ Y(j\omega) \end{bmatrix} = 0.$$

This system has a nontrivial solution only if its matrix determinant equals zero, that is,

$$1 + N(A,\omega)G(j\omega) = 0, \tag{2.15}$$

and the amplitudes and frequencies of the limit cycles can be estimated by the solutions of (2.15), which is known as the harmonic balance (HB) equation.

2.4.3 Loeb's Stability Criterion

Under small amplitude or frequency perturbations, a limit cycle is said to be stable if the trajectories of a system are attracted back towards the cycle. On the other hand, if the amplitude or frequency grows or decays leading the trajectories away from the limit cycle, it is said to be unstable. The stability of a limit cycle can be determined in terms of the DF-characterized system via an analytical method devised by Loeb (1956, as cited in Gelb & Vander Velde, 1968), such method relies on the assumption that the HB equation remains valid at some small deviations from the periodic solution given by A_0 and ω_0 (Boiko, 2018). Therefore, by taking

$$\begin{aligned} A_0 &\to A_0 + \Delta A, \\ \omega_0 &\to \omega_0 + \Delta\omega - j\Delta\sigma, \end{aligned} \tag{2.16}$$

into (2.15), the following equation must hold:

$$1 + N(A_0 + \Delta A,\ \omega_0 + \Delta\omega + j\Delta\sigma)G(j\omega_0 + j\Delta\omega + \Delta\sigma) = 0 \tag{2.17}$$

where ΔA is the amplitude deviation, $\Delta\omega$ is the frequency deviation, and $\Delta\sigma$ is the rate of change of amplitude, that is, $\Delta\sigma = \dot{A}/A$ (Gelb & Vander Velde, 1968).

Based on the referred assumption, a necessary condition for the stability of a limit cycle can be obtained as the following inequality, commonly known as the Loeb's criterion:

$$\frac{\partial U}{\partial A}\frac{\partial V}{\partial \omega} - \frac{\partial U}{\partial \omega}\frac{\partial V}{\partial A} > 0 \tag{2.18}$$

where the terms U and V are obtained from the HB equation as

$$\begin{aligned} U(A,\omega) &= \mathrm{Re}\left\{N(A,\omega) + G(j\omega)^{-1}\right\}, \\ V(A,\omega) &= \mathrm{Im}\left\{N(A,\omega) + G(j\omega)^{-1}\right\}. \end{aligned}$$

2.5 Lyapunov Stability for Generalized Forms

Stability theory is one of the main cornerstones for the analysis of nonlinear systems. Regarding the notion of stability in the sense of Lyapunov, recall the following statement (Khalil, 2002): Consider the autonomous system

$$\dot{x} = f(x) \tag{2.19}$$

where $f : D \to \mathbb{R}^n$ is a continuous map from a domain $D \subset \mathbb{R}^n$ into $\mathbb{R}^n$ and assume that the system has an equilibrium point at the origin, that is, $f(x)$ satisfies $f(0) = 0$. Then, the equilibrium point $x = 0$ of (2.19) is said to be

- stable if, for each $\varepsilon > 0$, there is $\delta = \delta(\varepsilon) > 0$ such that

$$||x(0)|| < \delta \Rightarrow ||x(t)|| < \varepsilon,\ \forall t \geq 0,$$

- unstable if not stable,
- asymptotically stable if it is stable and δ can be chosen such that

$$||x(0)|| < \delta \Rightarrow \lim_{t\to\infty} x(t) = 0. \tag{2.20}$$

Accordingly, one of the main results concerning Lyapunov stability can be stated by the following theorem:

Theorem 2.5.1 (Khalil, 2002) *Let $x = 0$ be an equilibrium point for the system (2.19) and $D \subset \mathbb{R}^n$ be a domain containing $x = 0$. Let $V : D \to \mathbb{R}$ be a continuously differentiable function such that*

$$V(0) = 0 \quad and \quad V(x) > 0 \quad in \quad D \setminus \{0\} \tag{2.21}$$

and

$$\dot{V}(x) \leq 0 \quad in \quad D. \tag{2.22}$$

Then, $x = 0$ is stable. Moreover, if

$$\dot{V}(x) < 0 \quad in \quad D \setminus \{0\}, \tag{2.23}$$

then, $x = 0$ is asymptotically stable.

2.5.1 Lyapunov Stability for Homogeneous Systems

In the case of homogeneous systems, such property gives rise to some additional features related to the stability of the equilibrium. Some of the main features include the ensurance of global asymptotic stability for a locally attractive equilibrium (Zubov, 1964), the existence of a homogeneous continuous LF for systems with globally asymptotically stable origin (Zubov, 1964), and the finite-time stability implied by the asymptotic one for a system with negative homogeneity degree (Bhat & Bernstein, 1997). Likewise, these results can be generalized for the case of DIs as shown in Bernuau et al. (2013). Therefore, such stability features still hold for systems with discontinuous right-hand side like the 2-RED. This is a powerful result that proves to be very useful for the analysis and design of homogeneous SMC systems and justifies great part of the antecedents on which this work is grounded.

2.5.2 Construction of Lyapunov Functions for Generalized Forms

Homogeneous polynomial functions are conventionally called forms (Lang, 2002). A generalization based upon this notion of classical forms, comprising functions with polynomial structure but allowing real powers and preserving the sign of variables, lead to the concept of the so-called generalized forms (GFs). In agreement with Sanchez et al. (2016), a function $f : \mathbb{R}^n \to \mathbb{R}$ is a GF if it is r-homogeneous of degree m with weights $r = \begin{bmatrix} r_1 & \dots & r_n \end{bmatrix}^\top$ and exclusively consists of sums and products of terms of the type $a\lceil x_i \rfloor^p$ and $b\,|x_i|^q$, such that $a, b \in \mathbb{R}$ and $p, q \in \mathbb{Q}$.

In 2019, Sanchez and Moreno proposed a design methodology of LFs for a class of homogeneous systems described by GFs. According to their work, consider the system

$$\dot{x} = f(x;k), \quad x \in \mathbb{R}^n, \quad k \in \mathbb{R}^p \tag{2.24}$$

where k represents the vector of system free parameters and $f = \begin{bmatrix} f_1 & \dots & f_n \end{bmatrix}^\top$ is homogeneous with each function $f_i,\ i = 1, \dots, n$ being a GF with rational exponents. Moreover, let $V : \mathbb{R}^n \to \mathbb{R}$ be a GF corresponding to a LF for (2.24) and likewise, $W : \mathbb{R}^n \to \mathbb{R}$, a function of its derivative given by

$$W(x) = -\frac{\partial V(x)}{\partial x} f(x). \tag{2.25}$$

Thus, such methodology conveys some guidelines to construct a family of LF candidates $V(x;\alpha)$ and their respective $W(x;\beta)$, where α and β represent the vector of coefficients of the GFs monomials. In addition, it provides a systematic approach to find a matching set of coefficients α, β and parameters k, such that V and W are rendered positive definite (PD). This approach yields a useful tool for the design of systems constituted by GF such as SMC algorithms.

Although no LF for the 2-RED is designed from scratch in this work, this methodology is applied to tackle an intermediate problem; namely, given a set of parameters k, to find some suitable coefficients α which yield a LF from a given candidate family $V(x;\alpha)$. Briefly, this approach requires both GFs V and W to be transformed into a set of classical forms via a change of coordinates. If a solution α which renders all those forms PD is found, the positive definiteness of the original GFs follows thereafter, consequently demonstrating V to be a LF.

2.6 Positive Definiteness of Forms

Since the design methodology described in the previous section involves the demonstration of positive definiteness of a set of forms, Sanchez and Moreno (2019) suggested two approaches to perform this task: one relying on the use of a theorem by Pólya (1927, as cited in Hardy et al., 1988), and the other one via a representation of such forms as a sum of squares (SOS).

The SOS approach is the one used in this work; therefore, it is briefly introduced.

2.6.1 Sum of Squares Representation

Based on the work by Parrilo (2000), whereby the SOS decomposition for multivariable polynomials can be formulated as a linear matrix inequality (LMI), the nonnegativity of a form can be verified by proving it to be a SOS. Accordingly, let $F : \mathbb{R}^n \to \mathbb{R}$ be a classical form of degree $2m, m \in \mathbb{Z}_{>0}$, then F is said to be a SOS if there exist a finite number of forms $f_i,\ i = 1, 2, \dots, N$ such that

$$F(x) = \sum_{i=1}^{N} \left[f_i(x)\right]^2. \tag{2.26}$$

It can be seen that F is positive semidefinite if it is a SOS. Furthermore, if

$$\widetilde{F}(x) = F(x) - \theta \sum_{j=1}^{n} x_j^{2m} \tag{2.27}$$

is a SOS for some $\theta \in \mathbb{R}_{>0}$, then F is PD (Papachristodoulou & Prajna, 2002). Thus, the SOS approach provides with a sufficient condition to prove the positive definiteness of a form, task which can be performed via some specialized software such as SOSTOOLS (Prajna et al., 2002).

Chapter 3

Gain Design of the 2-RED

3.1 Assumptions

In order to study the behavior of the differentiator output under the presence of a time delay, the 2-RED system is considered as depicted in Fig. 3.1. From the figure it can be observed that the differentiator nonlinearites can be lumped into one single block which in turn can be replaced by its corresponding DF. On the other hand, if the input is set as $f(t) = 0$ and a first-order approximation is used for the time delay so that it can be grouped with the integrator into a linear block, a closed loop with the structure shown in Fig. 2.3 can be attained. Furthermore, it is asumed that the input at the nonlinear block is a sinusoidal signal and that the linear element fulfils the filtering hypothesis.

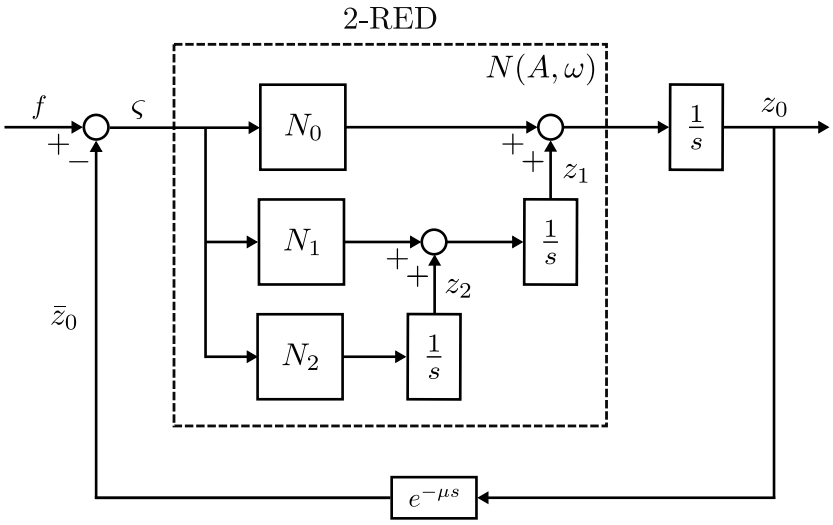

Figure 3.1: Second order robust exact differentiator DF diagram.

These assumptions meet the requirements imposed by the DF approach described in the previous chapter, allowing the use of that technique. Although such assumptions may raise no objection to the application of this technique to the study of stabilizing controllers, as done by Pérez-Ventura and Fridman (2019a) for example, its use to the considered differentation scheme may bring up some uncertainties specially with regard to the requirement of a reference or input signal $f(t) = 0$.

Since such restriction would limit the differentiator to solely take the zero function as the input signal to be differentiated, such results would turn to be little useful in practice. Nevertheless, this approach is based on the assumption of a nonideal sliding mode whose motion comprises well discernible slow and fast components. Therefore, such motion may be studied as arising from two separate dynamic subsystems; namely, the slow one dealing with the motion due to nonzero initial conditions and forced responses caused by an input signal or a disturbance, and the fast one corresponding to the self-excited oscillations due to the *chattering* phenomenon. Accordingly, the slow subsystem would be related to the motion along the sliding surface, whereas the fast one, with that across the surface. This decomposition of the dynamics results appropriate on account of the assumption that the external input is much slower than the self-excited oscillations, which is usually the case in real sliding modes, allowing to study the fast component of motion due to *chattering* via the DF method (Boiko, 2005); more accurate results may be obtained by using a more sofisticated approach such as the LPRS method (Boiko, 2003) or the dual-input describing function (DIDF) (Gelb & Vander Velde, 1968), though.

With respect to the issue of how slow must external signals be in comparison with the self oscillations, Boiko (2005) states the nonrigorous definition that the external signal can be regarded comparatively slow if it can be considered constant over the oscillations period without significant loss of accuracy of the oscillations estimation. In agreement with such notion and recalling Fig. (2.2), with a nonzero input in this case, Gelb and Vander Velde (1968) give the following condition as an assumption for the formulation of the DIDF:

$$T\left|r'(t)\right| \ll A \tag{3.1}$$

where T and A are the period and amplitude of the limit cycle oscillation at the input of the nonlinearity, respectively, and r is an external slowly-varying reference input, that is, one which changes relatively little with respect to A over the period T. Therefore, the results obtained in this work based on the assumption of a zero function at the input may only hold valid for low-frequency nonzero reference inputs $r(t)$ satisfying (3.1) along with the *chattering* parameters A and T.

3.2 Steady State Oscillatory Response: Existence and Parameters

In oder to compute the parameters of the estimated *chattering* oscillations caused by the delay as a function of the differentiator gains, it is first required to determine the DF of the nonlinearities and the transfer function of the linearities. Then the HB equation can be stated and solved for the sought oscillation parameters in terms of the differentiator gains. Such expressions are later used along Loeb's criterion to introduce a gain selection methodology ensuring stable oscillations with a local minimum amplitude. Thus, let $\varsigma = \bar{z}_0 - f(t)$ denote the input to the differentiator nonlinear block under the presence of a delay. From Fig. 3.1 it can be noticed that the 2-RED system (2.5) can be regarded as formed by a parallel interconnection involving nonlinearities of the type $k_i\lceil\varsigma^{(q)}\rfloor^p$ with $p \in \mathbb{Z}_{\geq 0}$ and $q \in \mathbb{Q}_{\geq 0}$. Therefore, if the DF of this kind of nonlinearities is known, then a DF for the whole 2-RED can be easily computed accordingly.

3.2.1 Describing Function Computation

Under the assumption of a steady-state periodic response and the linear block satisfying the filtering hypothesis, ς can be approximated by its first harmonic as

$$\varsigma = A\sin(\omega t) \tag{3.2}$$

so, according to Pérez-Ventura and Fridman (2019b), the DF of a nonlinearity $k_i\lceil\varsigma^{(q)}\rfloor^p$ is given by

$$N_i(A,\omega) = j^q\omega^{pq}\frac{2k_i}{\pi A^{1-p}}\int_0^\pi \lceil\sin(\omega t)\rfloor^p \mathrm{d}\omega t. \tag{3.3}$$

Next, consider the B and Γ functions defined as

$$\mathrm{B}(x,y) = 2\int_0^{\pi/2} (\sin\theta)^{2x-1}\,(\cos\theta)^{2y-1}\,\mathrm{d}\theta \tag{3.4}$$

and

$$\Gamma(z) = \int_0^\infty x^{z-1}e^{-x}\mathrm{d}x \tag{3.5}$$

where x, y and z are complex inputs with positive real part. Due to the relationship among these functions given by

$$\mathrm{B}(x,y) = \frac{\Gamma(x)\Gamma(y)}{\Gamma(x+y)} \tag{3.6}$$

and further properties of the Γ function (see Beals & Wong, 2010, for more details), the DF (3.3) can be computed as

$$N_i(A,\omega) = j^q\omega^{pq}\frac{2k_i}{\sqrt{\pi}A^{1-p}}\frac{\Gamma\left(\frac{p}{2}+1\right)}{\Gamma\left(\frac{p}{2}+\frac{3}{2}\right)}. \tag{3.7}$$

Therefore, the DF of the 2-RED can be obtained from the DF of the three individual nonlinearities corresponding with each of the gains k_0, k_1 and k_2 as

$$N(A,\omega) = N_0 + \frac{1}{j\omega}N_1 + \frac{1}{(j\omega)^2}N_2. \tag{3.8}$$

Thus, evaluating (3.7) for the values of p and q in Table 3.1, corresponding to each nonlinear term of the 2-RED, the DFs are obtained as

$$N_0 = \frac{2\delta_0 k_0}{\pi A^{1/3}}, \tag{3.9a}$$

$$N_1 = \frac{2\delta_1 k_1}{\pi A^{2/3}}, \tag{3.9b}$$

$$N_2 = \frac{4k_2}{\pi A}, \tag{3.9c}$$

where δ_0 and δ_1 are introduced for the sake of simplicity as

$$\delta_1 = \sqrt{\pi}\frac{\Gamma\left(\frac{7}{6}\right)}{\Gamma\left(\frac{5}{3}\right)} \quad \text{and} \quad \delta_0 = \sqrt{\pi}\frac{\Gamma\left(\frac{4}{3}\right)}{\Gamma\left(\frac{11}{6}\right)}.$$

N_i	p	q
N_0	2/3	0
N_1	1/3	0
N_2	0	0

Table 3.1: Exponents and derivative order values for each nonlinearity conforming the 2-RED.

Finally, from (3.8) and (3.9), the DF of the 2-RED results in

$$N(A,\omega) = \frac{2\delta_0 k_0}{\pi A^{1/3}} - \frac{4k_2}{\pi A\omega^2} - j\frac{2\delta_1 k_1}{\pi A^{2/3}\omega}. \tag{3.10}$$

3.2.2 Steady State Oscillation Parameters

Besides the DF, the transfer function of the linear block is required to compute the HB whose solution yields the approximated oscillation parameters. Thus, in order to group the time delay and the integrator together into the linear block, a first order Padé approximation (Baker et al., 1996) is used as

$$e^{-\mu s} \approx \frac{2-\mu s}{2+\mu s}. \tag{3.11}$$

Thus, including the integrator, the transfer function of the considered linear element is given by

$$G(s) = \frac{2-\mu s}{s\,(2+\mu s)}. \tag{3.12}$$

Finally, substituting (3.10) and (3.12) into (2.15), the HB equation for the 2-RED results in

$$\frac{2\delta_0 k_0}{\pi A^{1/3}} - \frac{4k_2}{\pi A\omega^2} - j\frac{2\delta_1 k_1}{\pi A^{2/3}\omega} = \frac{4\mu\omega^2}{4+\mu^2\omega^2} - j\frac{\omega\left(4-\mu^2\omega^2\right)}{4+\mu^2\omega^2}. \tag{3.13}$$

Hence, in order to determine the steady state oscillation parameters, (3.13) can be separated into its real and imaginary parts. Accordingly, the amplitude can be estimated by solving the real part for A as

$$A = \mu^3\left[\frac{2\delta_1 k_1\left(4+\mathbb{K}^2\right)}{\pi\mathbb{K}^2\left(4-\mathbb{K}^2\right)}\right]^{\frac{3}{2}}, \tag{3.14}$$

whereas the frequency is given by

$$\omega = \frac{\mathbb{K}}{\mu}, \tag{3.15}$$

where the parameter $\mathbb{K}$ in (3.14) and (3.15) can be obtained by solving the equation resulting from substituting the amplitude (3.14) into the imaginary part of the HB equation (3.13); such resultant equation is given by

$$a\frac{k_0}{k_1^{1/2}}\left(4+\mathbb{K}^2\right) - b\frac{k_2}{k_1^{3/2}}\left(4-\mathbb{K}^2\right) = \mathbb{K}\left[\frac{4+\mathbb{K}^2}{4-\mathbb{K}^2}\right]^{\frac{1}{2}} \tag{3.16}$$

with

$$a = \left(\frac{\delta_0^2}{8\pi\delta_1}\right)^{\frac{1}{2}} \quad \text{and} \quad b = \left(\frac{\pi}{8\delta_1^3}\right)^{\frac{1}{2}}.$$

Once the oscillation parameters corresponding to the input to the nonlinear block, that is, $\bar{z}_0 = A\sin(\omega t)$, are known, upper bounds of the magnitude of the differentiator state variables can be estimated accordingly. First, based on the previously computed DFs, a first-order approximation of z_0, z_1 and z_2 can be obtained as

$$z_0 = -j\frac{N}{\omega}\bar{z}_0 = \left[-\frac{N_1}{\omega^2} + j\left(\frac{N_2}{\omega^3} - \frac{N_0}{\omega}\right)\right]\bar{z}_0, \tag{3.17a}$$

$$z_1 = \left(-\frac{N_2}{\omega^2} - j\frac{N_1}{\omega}\right)\bar{z}_0, \tag{3.17b}$$

$$z_2 = -j\frac{N_2}{\omega}\bar{z}_0. \tag{3.17c}$$

Then, substituting the corresponding DFs (3.9) in (3.17), the magnitude upper bounds can be estimated as

$$|z_0| = \left[\left(\frac{2\delta_1 k_1 A^{1/3}}{\pi\omega^2}\right)^2 + \left(\frac{4k_2 - 2\delta_0 k_0 A^{2/3}\omega^2}{\pi\omega^3}\right)^2\right]^{\frac{1}{2}}, \tag{3.18a}$$

$$|z_1| = \left[\left(\frac{4k_2}{\pi\omega^2}\right)^2 + \left(\frac{2\delta_1 k_1 A^{1/3}}{\pi\omega}\right)^2\right]^{\frac{1}{2}}, \tag{3.18b}$$

$$|z_2| = \frac{4k_2}{\pi\omega}. \tag{3.18c}$$

Furthermore, notice that $|\bar{z}_0| = A$ and that A is a function of both k_1 and $\mathbb{K}$. It is also important to remark that since the considered input is the zero signal $f(t) = 0$, the estimated upper bounds $|z_i|$, $i = 0, 1, 2$ coincide with the estimated oscillations amplitude.

3.2.3 Asymptotic Orbital Stability

For the purpose of introducing a gain selection criterion such that the chosen parameters give rise to orbital stable oscilations, a stability condition as a function of the differentiator gains can be obtained as follows. Recalling Loeb's Criterion and considering both the DF of the 2-RED (3.10) and the transfer function of the linear block (3.12), the inequality (2.18) yields the following stability condition:

$$k_1^{1/2} > \left(\frac{32\delta_0^2}{\pi\delta_1}\right)^{\frac{1}{2}} \left[\frac{\mathbb{K}\left(16-\mathbb{K}^4\right)^{1/2}}{\mathbb{K}^4+16\mathbb{K}^2+16}\right] k_0. \tag{3.19}$$

On the other hand, from the HB equation, solving (3.16) for k_0 leads to

$$k_0 = \frac{\mathbb{K}}{a\left(16-\mathbb{K}^4\right)^{1/2}} k_1^{1/2} + \frac{b\left(4-\mathbb{K}^2\right)k_2}{a\left(4+\mathbb{K}^2\right)k_1}. \tag{3.20}$$

Therefore, from (3.19) and (3.20), the stability condition can be restated in terms of k_2, k_1 and $\mathbb{K}$ as

$$k_1^{3/2} > \left[\frac{2^{5/2}\delta_0 b\mathbb{K}\left(4-\mathbb{K}^2\right)^{3/2}}{\left(4+\mathbb{K}^2\right)^{1/2}\left(\left(\pi\delta_1\right)^{1/2} a\left(\mathbb{K}^4+16\mathbb{K}^2+16\right)-2^{5/2}\delta_0\mathbb{K}^2\right)}\right] k_2. \tag{3.21}$$

In this way, (3.21) is used first to select k_1 and k_2 complying with the orbital stability condition, then the corresponding k_0 providing a suboptimal performance, that is, ensuring a local minimum amplitude, can be computed with (3.20).

3.3 Gain Design Methodology

Based on the methodology used in the study of some SMC algorithms such as the STC and the PID-CSMC (Pérez-Ventura & Fridman, 2019a; Pérez-Ventura et al., 2021), the proposed selection methodology of the gains for the 2-RED comprise the following tasks:

- compute a pair of gains k_1 and k_2 giving rise to stable oscillations,
- given the pair of gains k_1 and k_2 ensuring orbital stability, adjust the remaining parameter k_0 in order to minimize the oscillations amplitude across the estimates of either z_0 or z_1.

This tasks can be achieved via the following three steps conforming the proposed algorithm:

1. fix k_1 and k_2 which ensure orbital stability according to the Loeb's Criterion given by the inequality (3.21),
2. find a $\mathbb{K}$ which minimizes the desired criterion; namely, A in (3.14) or $|z_1|$ in (3.18b),
3. given the minimizing $\mathbb{K}$, compute k_0 in terms of k_1 and k_2 with (3.20).

Following this methodology it is possible to find a gain k_0 resulting in a set of parameters that yield a local minimum *chattering* amplitude of the first derivative estimate given a pair k_1 and k_2 complying with the orbital stability condition.

In order to exemplify it, the methodology is first shown for the case of minimizing $|\bar{z}_0|$, that is, the amplitude of the delayed estimate of the input signal $f(t)$.

3.3.1 Minimizing Gain for $|\bar{z}_0|$

According to the described methodology, in order to minimize $|\bar{z}_0|$, which coincides with A as given in (3.14) as a function of $\mathbb{K}$, a minimum is found for such function at

$$\mathbb{K}^2 = -4 + 2^{5/2} \approx 1.657 \tag{3.22}$$

which in turn can be substituted into (3.20) and (3.21) to yield

$$k_0 = \frac{k_1^{3/2} + 2(2 - 2^{1/2})bk_2}{2^{3/2}ak_1} \tag{3.23}$$

and

$$k_1^{3/2} > 0.42235k_2. \tag{3.24}$$

In this way, a pair k_1 and k_2 ensuring orbital stability can be selected with (3.24); in turn, a suboptimal k_0 can be computed for such pair with (3.23). Note that the minimizing value of $\mathbb{K}$ is given by a constant that must hold for any selection of the suboptimal parameters k.

3.3.2 Minimizing Gain for $|z_1|$

In order to minimize the oscillations amplitude across the first derivative estimate, the amplitude A given by (3.14) is substituted in the expression for $|z_1|$ in (3.18b), leading to a function of $\mathbb{K}$ for which a minimum value can be found at

$$\mathbb{K}^2 = \frac{2\delta_1^3 k_1^3 - 8\pi k_2^2 + 2\left(5\delta_1^6 k_1^6 + 8\pi\delta_1^3 k_1^3 k_2^2\right)^{1/2}}{\delta_1^3 k_1^3 - 2\pi k_2^2} \tag{3.25}$$

This expression, just as in the previous case, can be substituted first into (3.21) to yield an orbital stability condition for the selection of k_1 and k_2, and then into (3.20) to find a corresponding suboptimal gain k_0.

Note that given k_2, it is not as straightforward to select k_1 complying with the stability criteria as can be done when minimizing $|\bar{z}_0|$ via the inequality (3.24). Since the minimizing $\mathbb{K}$ is a function of both k_1 and k_2, the suggested approach is to fix such pair of parameters and compute the respective $\mathbb{K}$ with (3.25), then verify the feasibility of such selection via the inequality (3.21). Having attained an appropriate selection of k_1 and k_2, k_0 can be directly determined with (3.20), though.

3.4 Numeric Examples

In order to test the methodology, some sets of suboptimal gains can be found based on preexisting suggested parameters for the 2-RED taken from the literature review. Accordingly, Table 3.2 shows

Set	k_0	k_1	k_2	Reference
I	3.1	5.0	1.01	Sanchez, Cruz-Zavala, et al., 2018
II	6.0	5.0	0.2	Sanchez et al., 2016
III	3.45	5.65	1.1	Cruz-Zavala and Moreno, 2018
IV	4.44	5.75	0.5	Moreno, 2012
V	9.56	6.87	0.02	Ortiz-Ricardez et al., 2015

Table 3.2: Preexisting 2-RED gains sets found in the literature.

some reported sets of gains taken from previous works developed after a LF for the differentiator was introduced for the first time by Moreno (2012).

Now, assuming a delay with $\mu = 0.01$, the proposed selection algorithm can be applied in order to determine some gain sets minimizing the estimated oscillations amplitude for either z_0 or z_1. For the case of z_0, first k_1 and k_2 are selected as given in Table 3.2 for each of the parameter sets and it is verified that they satisfy with the stability condition (3.24). Then, the parameter $\mathbb{K}$ minimizing the amplitude of the estimated oscillations across z_0 is taken as (3.22). Finally, the remaining gain k_0 is computed from (3.23) with the corresponding values of k_1, k_2 and $\mathbb{K}$.

For the case of z_1, since the stability condition (3.21) involves both gains k_1, k_2 and the parameter $\mathbb{K}$, the value of $\mathbb{K}$ minimizing the amplitude of the estimated oscillations across z_1 is first computed from (3.25) with the values of k_1 and k_2 as given for each of the parameter sets in Table 3.2. Then, the stability condition (3.21) is now verified for each pair k_1, k_2 and the corresponding parameter $\mathbb{K}$. Finally, the remaining gain k_0 is computed from (3.20) with the determined values of k_1, k_2 and $\mathbb{K}$.

It should be noticed that for the case of z_1, the first and second steps of the design methodology from Section 3.3 were swapped due to the fact that the corresponding stability condition includes explicitely the parameter $\mathbb{K}$, while for the case of z_1 it just depends on k_1 and k_2. Nevertheless, the tasks to be achieved by the methodology are well fulfilled for both cases. Namely, ensuring stable oscillations from the pair of gains k_1 and k_2, and adjusting the remaining parameter k_0 so that the desired oscillations amplitude is minimized. Hence, the corresponding sets of parameters obtained via the proposed methodology are shown in Tables 3.3 and 3.4 for the cases of minimizing the oscillations amplitude for z_0 and z_1, respectively.

Set	k_0	k_1	k_2
I	3.23	5.0	1.01
II	3.2	5.0	0.2
III	3.46	5.65	1.1
IV	3.44	5.75	0.5
V	3.73	6.87	0.02

Table 3.3: Suboptimal 2-RED gains sets for minimal $|\bar{z}_0|$.

Following, some examples illustrating the predicted performance rendered by one of such sets of suboptimal parameters sets are presented in comparison with actual results taken from simulations for the 2-RED.

Set	k_0	k_1	k_2
I	4.55	5.0	1.01
II	4.5	5.0	0.2
III	4.83	5.65	1.1
IV	4.84	5.75	0.5
V	5.27	6.87	0.02

Table 3.4: Suboptimal 2-RED gains sets for minimal $|z_1|$.

3.4.1 Zero Function

The steady-state performance of the differentiator for the determined gains can be depicted with a graph such as that in Fig. 3.2 for the parameters set I in Tables 3.2-3.4, where for a given delay μ and a fixed pair k_1 and k_2, the oscillations amplitude are plotted against k_0. Both the estimated amplitude computed via the HB equation from (3.14) and that determined by computer simulation are shown in the blue and red curves, respectively. In accordance with the study assumptions, the zero function $f(t) = 0$ was considered to test the found suboptimal gains; therefore, the oscillations arise due to nonzero initial conditions of the differentiator error. With respect to the simulation results, two of them are distinguished: those considering the Padé approximant for the delay, and the others dismissing such approximation in the simulation. Moreover, the estimated amplitude corresponding to determined suboptimal gains are denoted with the black dots.

Additionally, in Figs. 3.3 - 3.5 the results from the simulation are plotted, showing the behavior of the differentiator states. The *chattering* phenomenon can be appreciated as the convergence of the trajectories to a limit cycle; accordingly, the amplitude values of such steady-state oscillations were the ones used in the plots in Fig. 3.2. It can also be seen from those figures that the higher the order of the derivative estimate, the higher the amplitude of the oscillations. Furthermore, from the detailed views, it can be observed that although the assumption of a sinusoid holds well for z_0, it weakens for z_1 and even more for z_2 for which the signal is rendered triangular. Therefore, the DF of the corresponding nonlinearity N_2 in (3.9c) can be corrected as

$$N_{2_{\text{corrected}}} = \frac{\pi k_2}{2A}. \tag{3.26}$$

Taking into account such correction in the corresponding expressions for the first order approximations of z_0, z_1 and z_2 given in (3.17), the magnitude upper bounds in (3.18) can be computed anew as

$$|z_0|_{\text{corrected}} = \left[\left(\frac{2\delta_1 k_1 A^{1/3}}{\pi\omega^2} \right)^2 + \left(\frac{\pi^2 k_2 - 4\delta_0 k_0 A^{2/3}\omega^2}{2\pi\omega^3} \right)^2 \right]^{\frac{1}{2}}, \tag{3.27a}$$

$$|z_1|_{\text{corrected}} = \left[\left(\frac{\pi k_2}{2\omega^2} \right)^2 + \left(\frac{2\delta_1 k_1 A^{1/3}}{\pi\omega} \right)^2 \right]^{\frac{1}{2}}, \tag{3.27b}$$

$$|z_2|_{\text{corrected}} = \frac{\pi k_2}{2\omega}. \tag{3.27c}$$

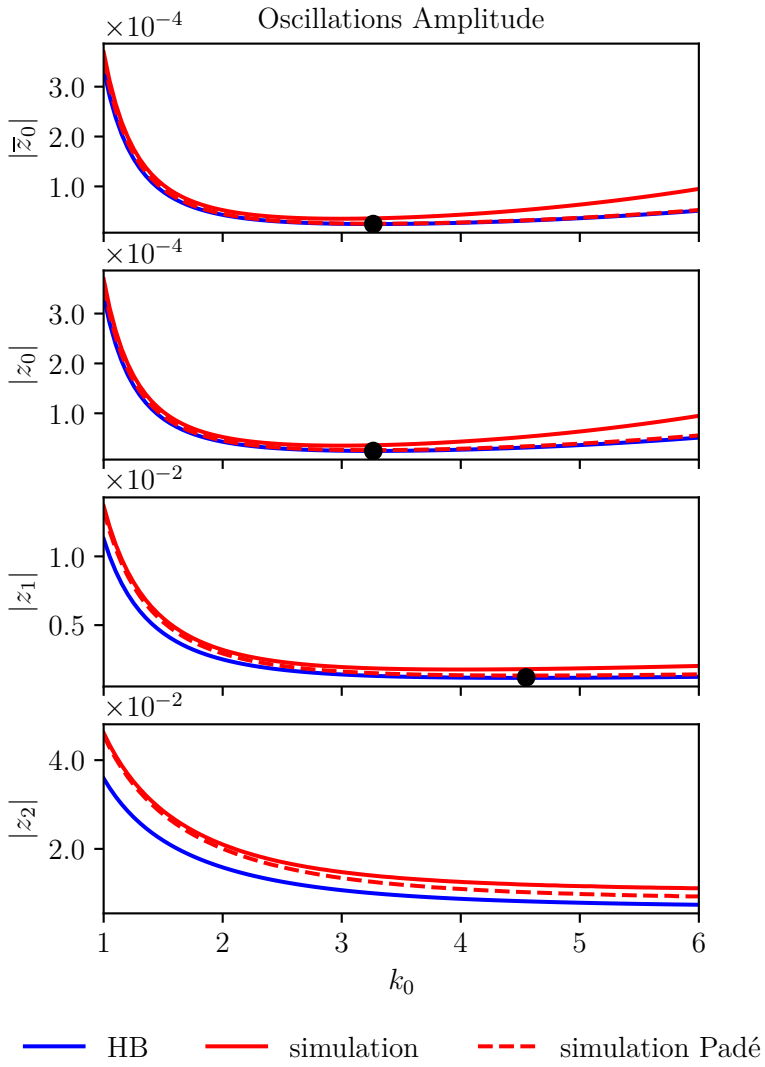

Figure 3.2: Steady-state response amplitude considering a delay $\mu = 0.01$ and the fixed pair $k_1 = 5.0$ and $k_2 = 1.01$ of gains set I from Tables 3.2-3.4, varying k_0.

By using the corrected upper bounds terms in (3.27), more accurate amplitude estimations can be obtained as seen from a comparison between the plots from Fig. 3.6 and the former one from Fig. 3.2; such improvement is less noticeable for $|z_0|$ and $|z_1|$ than for $|z_2|$, though. Nevertheless, a corresponding new expression for the $\mathbb{K}$ that minimizes the magnitude of the corrected term $|z_1|$ in (3.27b) could be obtained, and consequently, updated criteria for the selection of the suboptimal k_0 which minimizes the *chattering* amplitude of the first derivative estimate.

Introducing the detailed views of each of the subplots from Fig. 3.6 in Figs. 3.3 - 3.5, it can be seen that the estimations via the HB equation show a close agreement with the simulation results considering the Padé approximation. Therefore, the determined suboptimal gains set yields a minimum oscillation amplitude close to that achieved in the simulations. On the other hand, omitting the Padé approximant in the simulations, the prediction of the oscillations amplitude not only turns to be less effective, but also the minimum is attained with a gain k_0 lying further from

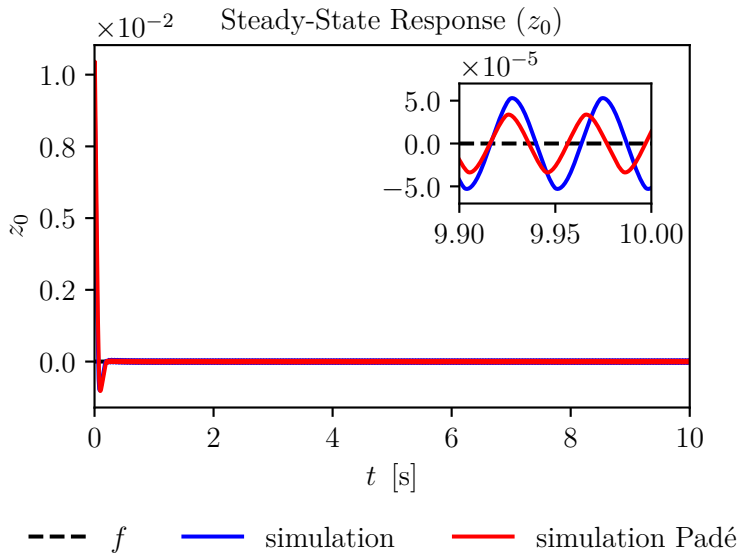

Figure 3.3: Simulation results for z_0 considering a delay $\mu = 0.01$ and the suboptimal gains of set I from Table 3.4.

the determined suboptimal one. Nonetheless, the plots show that the methodology yields consistent qualitative results in accordance with the considered assumptions and by using the other gains sets from Tables 3.3 and 3.4 alike results could be obtained.

3.4.2 Sinusoidal Function

Considering a more illustrative case where $f(t) \neq 0$, the sinusoidal function

$$f(t) = 0.5\sin(0.5t) + 0.5\cos(t)$$

was introduced to perform further simulations. Accordingly, the evolution of the differentiator states for both the cases with and without using the Padé approximant are shown in Fig. 3.10. It can be appreciated that under the presence of the delay, the differentiator no longer converges exactly to the base signal and its correspondent derivatives; this is particularly observed for the last state z_2.

Regarding the differentiation error, the plots from Figs. 3.11 and 3.12 show a detailed view of the first derivative error ε_1 for the two kinds of simulated cases, that is, with and without using the Padé approximation. Besides the suboptimal gains set, the results for other two sets of parameters with different values of k_0 are plotted in order to appreciate the performance of the differentiatior under such gain selection for a nonzero input signal. It can be appreciated that the curves describe small amplitude oscillations across low frequency sinusoids. Therefore, in order to extract the amplitude of such oscillations and make a graph such as that shown in Figs. 3.2 and 3.6, a further processing must be performed to the resultant signals from the simulations. Such plots might result helpful to better visualize the behavior of the differentiator for gains lying more closely to the suboptimal one. Nevertheless, from the simulated cases it seems that the results obtained under the zero function assumption may hold too for other kinds of signals as long as such inputs remain comparatively

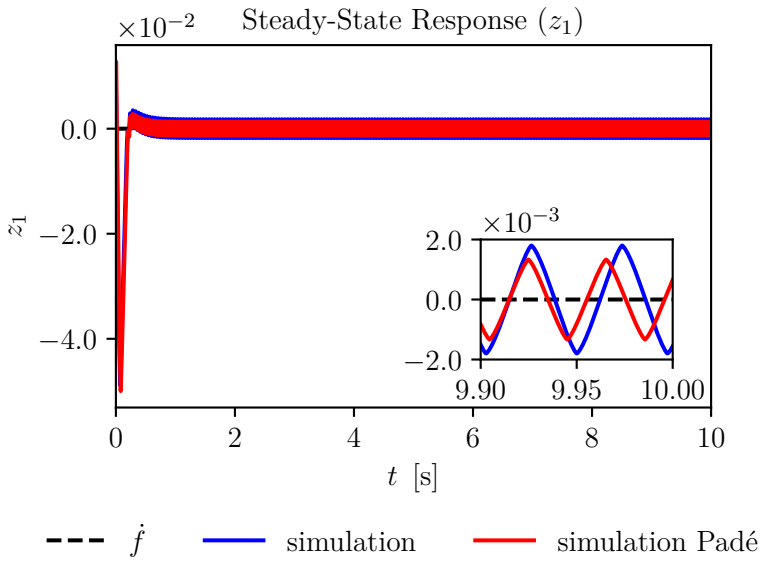

Figure 3.4: Simulation results for z_1 considering a delay $\mu = 0.01$ and the suboptimals gains of set I from Table 3.4.

slow in comparison with regard to the high-frequency oscillations.

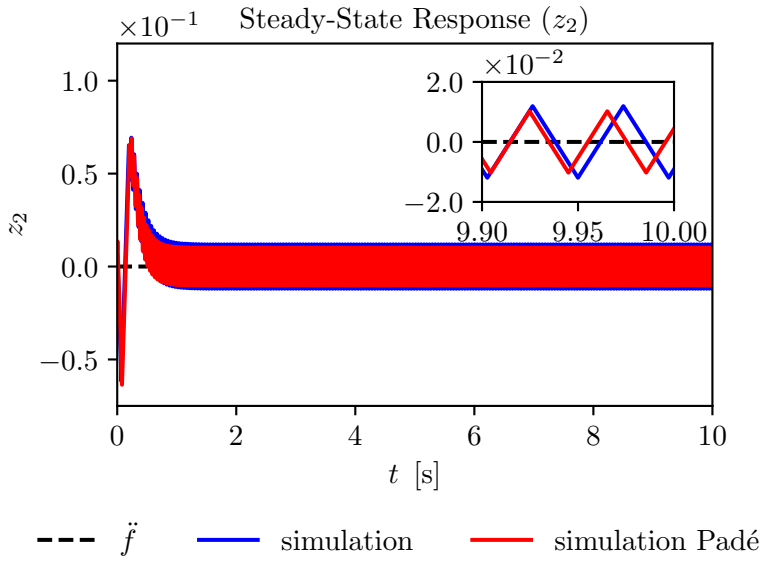

Figure 3.5: Simulation results for z_2 considering a delay $\mu = 0.01$ and the suboptimal gains of set I from Table 3.4.

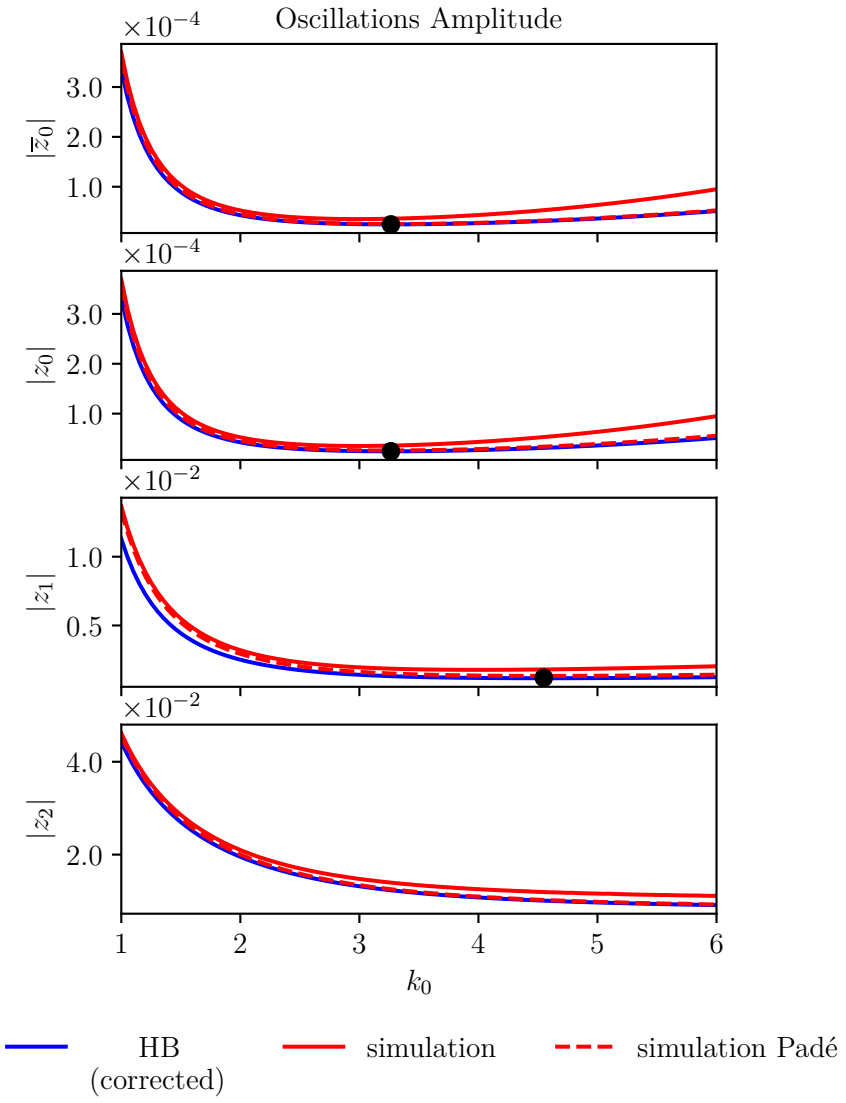

Figure 3.6: Steady-state response amplitude considering a delay $\mu = 0.01$ and the fixed pair $k_1 = 5.0$ and $k_2 = 1.01$ of gains set I from Tables 3.2-3.4, varying k_0; corrected terms due to the triangular signal are considered for the amplitude estimation via the HB equation.

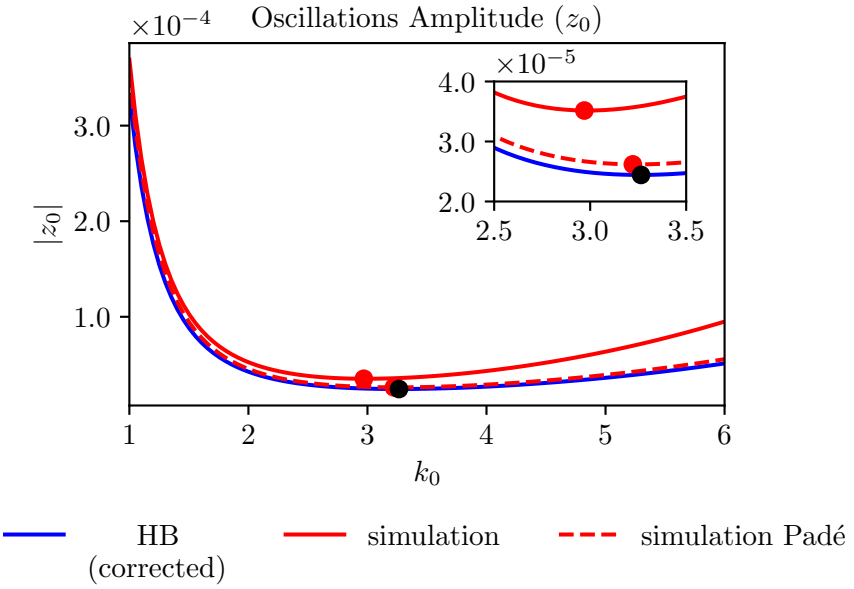

Figure 3.7: Steady-state response amplitude for z_0 considering a delay $\mu = 0.01$ and the fixed pair $k_1 = 5.0$ and $k_2 = 1.01$ of gains set I from Tables 3.2-3.4, varying k_0.

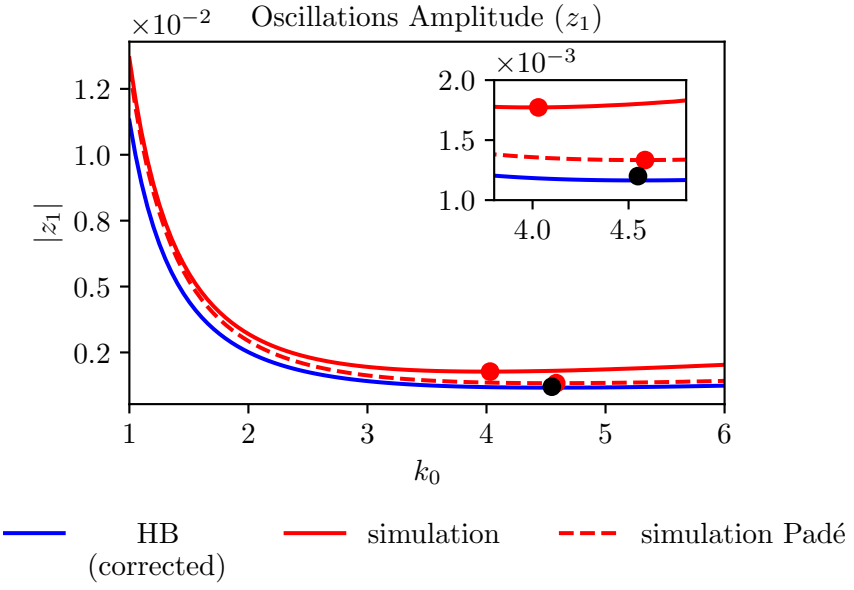

Figure 3.8: Steady-state response amplitude for z_1 considering a delay $\mu = 0.01$ and the fixed pair $k_1 = 5.0$ and $k_2 = 1.01$ of gains set I from Tables 3.2-3.4, varying k_0.

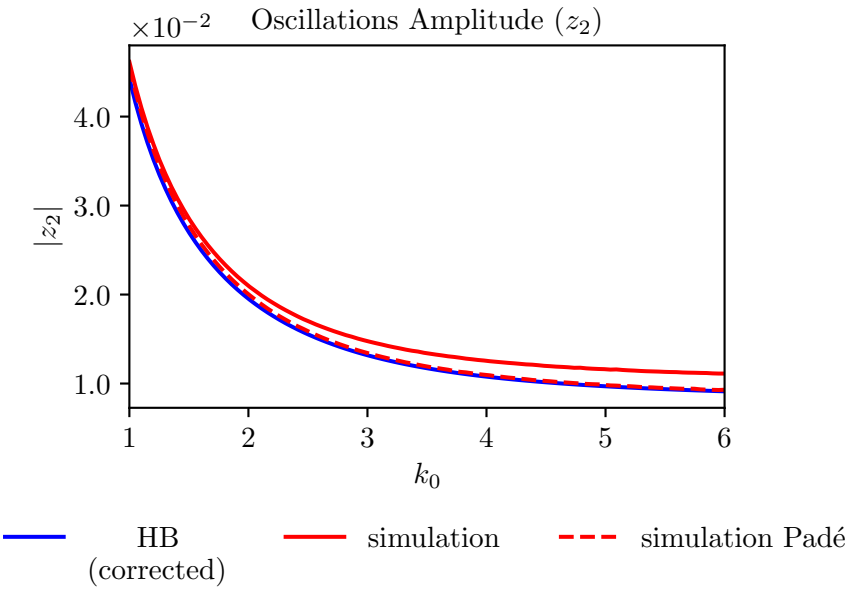

Figure 3.9: Steady-state response amplitude for z_2 considering a delay $\mu = 0.01$ and the fixed pair $k_1 = 5.0$ and $k_2 = 1.01$ of gains set I from Tables 3.2-3.4, varying k_0.

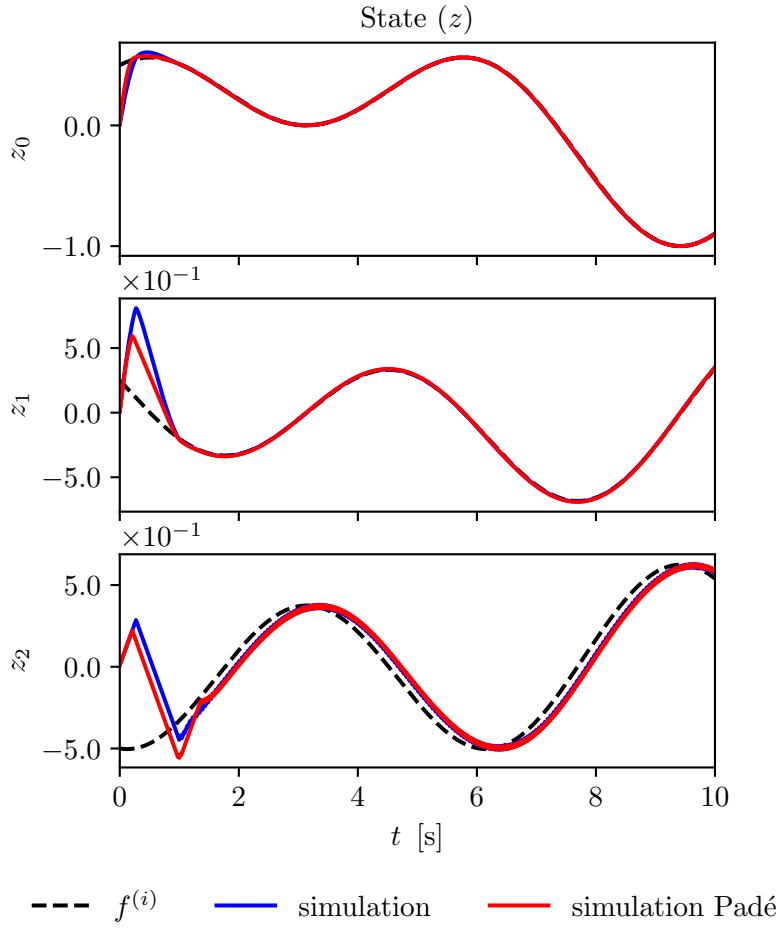

Figure 3.10: Simulation results considering a delay $\mu = 0.01$ and the suboptimal gains of set I from Table 3.4. $f(t) = 0.5\sin(0.5t) + 0.5\cos(t)$ is considered as input signal.

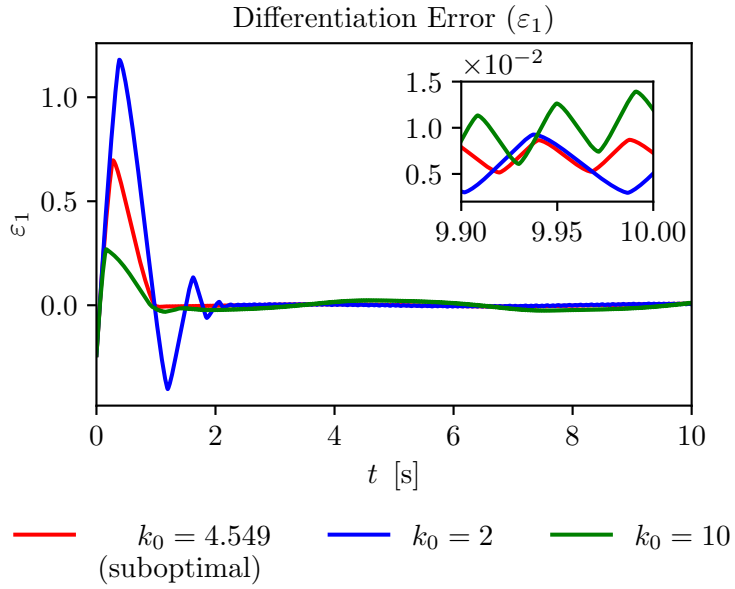

Figure 3.11: Simulation results for ε_1 considering a delay $\mu = 0.01$ and the suboptimal gains of set I from Table 3.4. The results for two additional gains sets with different values of k_0 are also plotted. $f(t) = 0.5\sin(0.5t) + 0.5\cos(t)$ is considered as input signal.

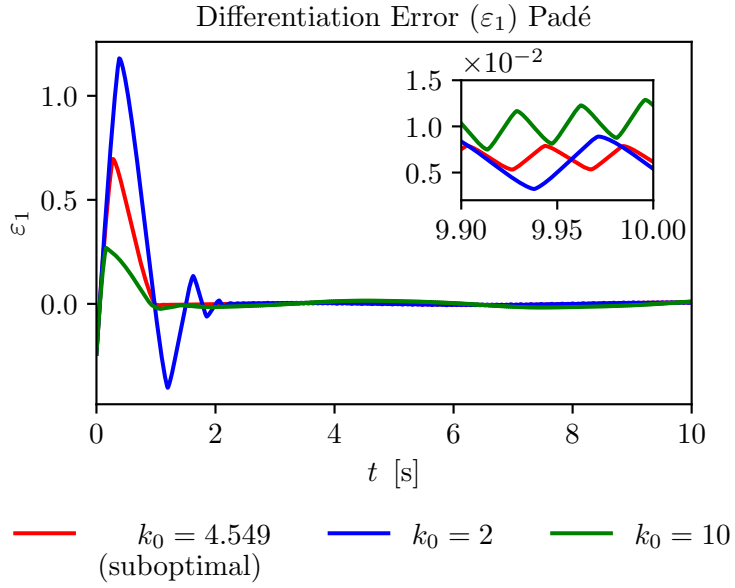

Figure 3.12: Simulation results for ε_1 considering a delay $\mu = 0.01$ using a Padé approximation and the suboptimal gains of set I from Table 3.4. The results for two additional gains sets with different values of k_0 are also plotted. $f(t) = 0.5\sin(0.5t) + 0.5\cos(t)$ is considered as input signal.

Chapter 4

Stability Analysis of the 2-RED

4.1 Stability Analysis for the Nominal Case

Even though a set of suboptimal gains like the ones presented on the previous chapter has been determined, a problem regarding the feasibility of that parameters still remains; namely, to prove that the differentiator preserves its properties of global asymptotic stability for such parameters. Although under the considered assumptions such gains sets ensure the existence of an orbitally stable periodic solution minimizing the amplitude of the *chattering*, this is only verified within a region where the approximation of the steady-state response given by its fundamental harmonic, as in (3.2), holds. Therefore, in agreement with the approach in Pérez-Ventura et al. (2021), the asymptotic stability of the error dynamics (2.6) is proved for the ideal case, that is, without considering the time delay in the scheme of Fig. 1.1. This can be done by using a pre-existing LF candidate such as the ones found in the reviewed literature. Furthermore, this is first done by considering the nominal case, that is, with $\psi(t) = 0$ in (2.6).

4.1.1 Lyapunov Function Candidate

Recall the error dynamics of the 2-RED introduced in Subsection 2.3.2

$$\begin{aligned} \dot{\varepsilon}_0 &= -k_0 \lceil \varepsilon_0 \rfloor^{\frac{2}{3}} + \varepsilon_1, \\ \dot{\varepsilon}_1 &= -k_1 \lceil \varepsilon_0 \rfloor^{\frac{1}{3}} + \varepsilon_2, \\ \dot{\varepsilon}_2 &= -k_2 \lceil \varepsilon_0 \rfloor^{0} + \psi(t), \end{aligned} \tag{4.1}$$

where $\varepsilon_i = z_i - f_0^{(i)}(t)$, $i = 0, 1, 2$ was defined as the differentiation error and the term $\psi(t) = -f_0^{(3)}(t)$ was considered as a disturbance. Assuming an input signal without noise; that is, $f(t) = f_0(t)$, Sanchez et al. (2016) proved

$$V(\varepsilon) = \alpha_0 |\varepsilon_0|^{\frac{5}{3}} - \alpha_{01}\varepsilon_0\varepsilon_1 + \alpha_1 |\varepsilon_1|^{\frac{5}{2}} + \alpha_{02} \lceil \varepsilon_0 \rfloor^{\frac{4}{3}} \varepsilon_2 - \alpha_{12}\varepsilon_1 \lceil \varepsilon_2 \rfloor^3 + \alpha_2 |\varepsilon_2|^5 \tag{4.2}$$

to be a LF for (4.1) for the nominal case without perturbation; that is, for $\psi(t) = 0$. In that work, some sets of coefficients $\alpha = \begin{bmatrix} \alpha_0 & \alpha_{01} & \alpha_1 & \alpha_{12} & \alpha_2 \end{bmatrix}^\top$ and the corresponding differentiator gains $k = \begin{bmatrix} k_0 & k_1 & k_2 \end{bmatrix}^\top$ were found via both the Pólya and the SOS methods.

Since a set of gains k can be found with the methodology presented in the previous chapter, the remaining problem consists in finding a set of coefficients α which renders (4.2) a LF for the error dynamics (4.1) considering the ideal case without time delay as well as an input function complying with the condition $f_0^{(3)}(t) = 0$. This problem can be tackled via the approach devised by Sanchez and Moreno (2019) introduced in Chapter 2 which comprises the following two stages:

1. determine a set of classical forms associated to the GFs corresponding to the LF candidate V and the derivative $W = -\dot{V}$,
2. find a set of coefficients α which guarantee the positive definiteness of the set of forms via the Pólya or SOS methods.

4.1.2 Associated Forms Computation

Since the image of a GF with rational exponents can be represented as the image of a set of classical forms, the problem of verifying its positive definiteness can be posed as that of proving the corresponding set of forms to be PD. Once this set of classical forms, commonly known as the associated forms (AFs) is found, some procedure such as the Pólya or SOS techniques mentioned in Chapter 2 can be used to verify its positive definiteness. In like manner, the same approach allows to determine the coefficients of a GF, such as the LF candidate (4.2), to render it PD.

Each form in the set of AFs can be obtained via a change of coordinates which serves two purposes; namely, to transform the former GF into another one with integer exponents, and to restrict its domain to the open positive hyperoctant $\mathcal{P}$. Just as the case of quadrants in $\mathbb{R}^2$, hyperoctants are the generalization of this concept to $\mathbb{R}^n$; therefore, $\mathcal{O}_\gamma$ and $\overline{\mathcal{O}}_\gamma$, $\gamma = 1, \ldots, 2^n$ denote the open and closed hyperoctants in $\mathbb{R}^n$, respectively. Accordingly, the open positive hyperoctant in $\mathbb{R}^n$ is denoted as $\mathcal{P} = \{x \in \mathbb{R}^n \mid x_i > 0, i = 1, \ldots, n\}$, whereas the closed one, as $\overline{\mathcal{P}}\,\{x \in \mathbb{R}^n \mid x_i \geq 0, i = 1, \ldots, n\}$.

Thus, let $f : \mathbb{R}^n \to \mathbb{R}$ be a GF with rational exponents, then for each of the hyperoctants in $\mathbb{R}^n$, a corresponding form $f_\gamma : \mathcal{P} \to \mathbb{R}$, $\gamma = 1, \ldots 2^n$ can be obtained as $f_\gamma = f \circ \phi_\gamma$, where $\phi_\gamma : \mathcal{P} \to \overline{\mathcal{O}}_\gamma$ is a homeomorphism given by

$$\phi_\gamma(\zeta) = \begin{bmatrix} \sigma_1 \lceil \zeta_1 \rfloor^{\iota_1} & \ldots & \sigma_n \lceil \zeta_n \rfloor^{\iota_n} \end{bmatrix}^\top \tag{4.3}$$

with $\iota_i \in \mathbb{Z}_{>0}$, $i = 1, \ldots, n$ selected appropriately in order to yield each f_γ a form with integer exponents and well defined homogeneity degree, and σ_i denoting the sign of x_i in the open hyperoctant $\mathcal{O}_\gamma$.

Finally, according with Sanchez and Moreno (2019), define $\overline{f}_\gamma : \overline{\mathcal{P}} \to \mathbb{R}$ as the extension of the form $f_\gamma : \mathcal{P} \to \mathbb{R}$, that is, the function defined for all $x \in \overline{\mathcal{P}}$ by using the same correspondence rule of f_γ, then the set $\{\overline{f}_\gamma\}$ corresponds to the AFs of f.

Hence, for the LF candidate (4.2) with $\varepsilon \in \mathbb{R}^3$, the following hyperoctants can be distinguished:

$$
\begin{aligned}
\mathcal{O}_1 &= \left\{\varepsilon \in \mathbb{R}^3 \mid \varepsilon_0 > 0, \varepsilon_1 > 0, \varepsilon_2 > 0\right\},\\
\mathcal{O}_2 &= \left\{\varepsilon \in \mathbb{R}^3 \mid \varepsilon_0 > 0, \varepsilon_1 > 0, \varepsilon_2 < 0\right\},\\
\mathcal{O}_3 &= \left\{\varepsilon \in \mathbb{R}^3 \mid \varepsilon_0 > 0, \varepsilon_1 < 0, \varepsilon_2 > 0\right\},\\
\mathcal{O}_4 &= \left\{\varepsilon \in \mathbb{R}^3 \mid \varepsilon_0 > 0, \varepsilon_1 < 0, \varepsilon_2 < 0\right\},\\
\mathcal{O}_5 &= \left\{\varepsilon \in \mathbb{R}^3 \mid \varepsilon_0 < 0, \varepsilon_1 < 0, \varepsilon_2 < 0\right\},\\
\mathcal{O}_6 &= \left\{\varepsilon \in \mathbb{R}^3 \mid \varepsilon_0 < 0, \varepsilon_1 < 0, \varepsilon_2 > 0\right\},\\
\mathcal{O}_7 &= \left\{\varepsilon \in \mathbb{R}^3 \mid \varepsilon_0 < 0, \varepsilon_1 > 0, \varepsilon_2 < 0\right\},\\
\mathcal{O}_8 &= \left\{\varepsilon \in \mathbb{R}^3 \mid \varepsilon_0 < 0, \varepsilon_1 > 0, \varepsilon_2 > 0\right\}.
\end{aligned}
\tag{4.4}
$$

Now, let $\mathcal{P} = \left\{\zeta \in \mathbb{R}^3 \mid \zeta_0 > 0, \zeta_1 > 0, \zeta_2 > 0\right\}$ denote the open positive hyperoctant and considering the sign of the components of ε in the hyperoctants (4.4), define the following change of coordinates $\phi_\gamma : \mathcal{P} \to \overline{\mathcal{O}}_\gamma$, $\gamma = 1, \ldots, 8$ computed from (4.3) as

$$
\begin{aligned}
\phi_1(\zeta) &= \begin{bmatrix}\lceil\zeta_0\rfloor^3 & \lceil\zeta_1\rfloor^2 & \lceil\zeta_2\rfloor\end{bmatrix}^\top,\\
\phi_2(\zeta) &= \begin{bmatrix}\lceil\zeta_0\rfloor^3 & \lceil\zeta_1\rfloor^2 & -\lceil\zeta_2\rfloor\end{bmatrix}^\top,\\
\phi_3(\zeta) &= \begin{bmatrix}\lceil\zeta_0\rfloor^3 & -\lceil\zeta_1\rfloor^2 & \lceil\zeta_2\rfloor\end{bmatrix}^\top,\\
\phi_4(\zeta) &= \begin{bmatrix}\lceil\zeta_0\rfloor^3 & -\lceil\zeta_1\rfloor^2 & -\lceil\zeta_2\rfloor\end{bmatrix}^\top,\\
\phi_5(\zeta) &= \begin{bmatrix}-\lceil\zeta_0\rfloor^3 & -\lceil\zeta_1\rfloor^2 & -\lceil\zeta_2\rfloor\end{bmatrix}^\top,\\
\phi_6(\zeta) &= \begin{bmatrix}-\lceil\zeta_0\rfloor^3 & -\lceil\zeta_1\rfloor^2 & \lceil\zeta_2\rfloor\end{bmatrix}^\top,\\
\phi_7(\zeta) &= \begin{bmatrix}-\lceil\zeta_0\rfloor^3 & \lceil\zeta_1\rfloor^2 & -\lceil\zeta_2\rfloor\end{bmatrix}^\top,\\
\phi_8(\zeta) &= \begin{bmatrix}-\lceil\zeta_0\rfloor^3 & \lceil\zeta_1\rfloor^2 & \lceil\zeta_2\rfloor\end{bmatrix}^\top.
\end{aligned}
\tag{4.5}
$$

Therefore, from the homeomorphism (4.5) and the LF candidate (4.2), the corresponding classical forms can be obtained as $V_\gamma = V \circ \phi_\gamma$, $\gamma = 1, \ldots, 8$ leading to

$$
\begin{aligned}
V_1(\zeta) = V_5(\zeta) &= \alpha_0\zeta_0^5 - \alpha_{01}\zeta_0^3\zeta_1^2 + \alpha_1\zeta_1^5 + \alpha_{02}\zeta_0^2\zeta_2 - \alpha_{12}\zeta_1^2\zeta_2^3 + \alpha_2\zeta_2^5,\\
V_2(\zeta) = V_6(\zeta) &= \alpha_0\zeta_0^5 - \alpha_{01}\zeta_0^3\zeta_1^2 + \alpha_1\zeta_1^5 - \alpha_{02}\zeta_0^2\zeta_2 + \alpha_{12}\zeta_1^2\zeta_2^3 + \alpha_2\zeta_2^5,\\
V_3(\zeta) = V_7(\zeta) &= \alpha_0\zeta_0^5 + \alpha_{01}\zeta_0^3\zeta_1^2 + \alpha_1\zeta_1^5 + \alpha_{02}\zeta_0^2\zeta_2 + \alpha_{12}\zeta_1^2\zeta_2^3 + \alpha_2\zeta_2^5,\\
V_4(\zeta) = V_8(\zeta) &= \alpha_0\zeta_0^5 + \alpha_{01}\zeta_0^3\zeta_1^2 + \alpha_1\zeta_1^5 - \alpha_{02}\zeta_0^2\zeta_2 - \alpha_{12}\zeta_1^2\zeta_2^3 + \alpha_2\zeta_2^5.
\end{aligned}
\tag{4.6}
$$

Note that due to the symmetry of V, it is just necessary to test positive definiteness of half the forms. Also, for simplicity, the notation expressing the extension of the resulting forms is omitted, that is, instead of $\overline{V}_\gamma$ the AFs are just denoted as V_γ. Likewise, for W given by

$$
\begin{aligned}
W(\varepsilon) = \beta_1|\varepsilon_0|^{\frac{4}{3}} - \beta_2\lceil\varepsilon_0\rfloor^{\frac{2}{3}}\varepsilon_1 + \beta_3\lceil\varepsilon_0\rfloor^{\frac{1}{3}}\lceil\varepsilon_1\rfloor^{\frac{3}{2}} + \beta_4|\varepsilon_1|^2 + \beta_5\varepsilon_0\varepsilon_2 - \beta_6|\varepsilon_0|^{\frac{1}{3}}\varepsilon_1\varepsilon_2\\
- \beta_7\lceil\varepsilon_1\rfloor^{\frac{3}{2}}\varepsilon_2 - \beta_8\lceil\varepsilon_0\rfloor^0\varepsilon_1|\varepsilon_2|^2 - \beta_9\lceil\varepsilon_0\rfloor^{\frac{1}{3}}\lceil\varepsilon_2\rfloor^3 + \beta_{10}^{\pm}|\varepsilon_2|^4
\end{aligned}
\tag{4.7}
$$

with

$$
\begin{aligned}
\beta_1 &= \frac{5}{3}\alpha_0 k_0 - \alpha_{01} k_1 + \alpha_{02}\left(k_2 - \lceil \varepsilon_0 \rfloor^0 \psi(t)\right), & \beta_6 &= \frac{4}{3}\alpha_{02}, \\
\beta_2 &= \frac{5}{3}\alpha_0 - \alpha_{01} k_0, & \beta_7 &= \frac{5}{2}\alpha_1, \\
\beta_3 &= \frac{5}{2}\alpha_1 k_1, & \beta_8 &= 3\alpha_{12}\left(k_2 - \lceil \varepsilon_0 \rfloor^0 \psi(t)\right), \\
\beta_4 &= \alpha_{01}, & \beta_9 &= \alpha_{12} k_1, \\
\beta_5 &= \alpha_{01} + \frac{4}{3}\alpha_{02} k_0, & \beta_{10} &= \alpha_{12} + 5\alpha_2\left(k_2 \lceil \varepsilon_0 \rfloor^0 \lceil \varepsilon_2 \rfloor^0 - \lceil \varepsilon_2 \rfloor^0 \psi(t)\right),
\end{aligned}
\tag{4.8}
$$

the set of AFs can be obtained as $W_\gamma = W \circ \phi_\gamma$, $\gamma = 1, \ldots, 8$ by taking $\psi(t) = 0$ in the corresponding coefficients β_1, β_8 and β_{10} in (4.8), leading to

$$
\begin{aligned}
W_1(\zeta) &= W_5(\zeta) \\
&= \beta_1\zeta_0^4 - \beta_2\zeta_0^2\zeta_1^2 + \beta_3\zeta_0\zeta_1^3 + \beta_4\zeta_1^4 + \beta_5\zeta_0^3\zeta_2 - \beta_6\zeta_0\zeta_1^2\zeta_2 - \beta_7\zeta_1^3\zeta_2 - \beta_8\zeta_1^2\zeta_2^2 - \beta_9\zeta_0\zeta_2^3 + \beta_{10}^+\zeta_2^4, \\
W_2(\zeta) &= W_6(\zeta) \\
&= \beta_1\zeta_1^4 - \beta_2\zeta_0^2\zeta_1^2 + \beta_3\zeta_0\zeta_1^3 + \beta_4\zeta_1^4 - \beta_5\zeta_0^3\zeta_2 + \beta_6\zeta_0\zeta_1^2\zeta_2 + \beta_7\zeta_1^3\zeta_2 - \beta_8\zeta_1^2\zeta_2^2 + \beta_9\zeta_0\zeta_2^3 + \beta_{10}^-\zeta_2^4, \\
W_3(\zeta) &= W_7(\zeta) \\
&= \beta_1\zeta_1^4 + \beta_2\zeta_0^2\zeta_1^2 - \beta_3\zeta_0\zeta_1^3 + \beta_4\zeta_1^4 + \beta_5\zeta_0^3\zeta_2 + \beta_6\zeta_0\zeta_1^2\zeta_2 + \beta_7\zeta_1^3\zeta_2 + \beta_8\zeta_1^2\zeta_2^2 - \beta_9\zeta_0\zeta_2^3 + \beta_{10}^+\zeta_2^4, \\
W_4(\zeta) &= W_8(\zeta) \\
&= \beta_1\zeta_1^4 + \beta_2\zeta_0^2\zeta_1^2 - \beta_3\zeta_0\zeta_1^3 + \beta_4\zeta_1^4 - \beta_5\zeta_0^3\zeta_2 - \beta_6\zeta_0\zeta_1^2\zeta_2 - \beta_7\zeta_1^3\zeta_2 + \beta_8\zeta_1^2\zeta_2^2 + \beta_9\zeta_0\zeta_2^3 + \beta_{10}^-\zeta_2^4,
\end{aligned}
\tag{4.9}
$$

where

$$
\beta_{10}^+ = \alpha_{12} + 5\alpha_2 k_2 \quad \text{and} \quad \beta_{10}^- = \alpha_{12} - 5\alpha_2 k_2.
$$

4.1.3 Positive Definiteness Verification

In order to determine the set of coefficients α for which the sets of AFs $\{V_i\}$ and $\{W_i\}$ are PD and, consequently, show that (4.2) is a LF, the SOS procedure can be applied. Recall from Chapter 2, that this approach requires the forms to be of even degree. Therefore, the following change of coordinates can be introduced to comply with this requirement

$$
\zeta = \begin{bmatrix} \eta_1^2 & \eta_2^2 & \eta_3^2 \end{bmatrix}^\top. \tag{4.10}
$$

After applying the change of coordinates (4.10) and introducing the parameter θ, the set of AFs (4.6), can be brought to a structure suitable for the SOS approach, resembling that given by (2.27). Hence, for the set $\{V_i\}$ we obtain

$$
\begin{aligned}
\widetilde{V}_1(\eta) &= (\alpha_0-\theta)\eta_0^{10} - \alpha_{01}\eta_0^6\eta_1^4 + (\alpha_1-\theta)\eta_1^{10} + \alpha_{02}\eta_0^8\eta_2^2 - \alpha_{12}\eta_1^4\eta_2^6 + (\alpha_2-\theta)\eta_2^{10},\\
\widetilde{V}_2(\eta) &= (\alpha_0-\theta)\eta_0^{10} - \alpha_{01}\eta_0^6\eta_1^4 + (\alpha_1-\theta)\eta_1^{10} - \alpha_{02}\eta_0^8\eta_2^2 + \alpha_{12}\eta_1^4\eta_2^6 + (\alpha_2-\theta)\eta_2^{10},\\
\widetilde{V}_3(\eta) &= (\alpha_0-\theta)\eta_0^{10} + \alpha_{01}\eta_0^6\eta_1^4 + (\alpha_1-\theta)\eta_1^{10} + \alpha_{02}\eta_0^8\eta_2^2 + \alpha_{12}\eta_1^4\eta_2^6 + (\alpha_2-\theta)\eta_2^{10},\\
\widetilde{V}_4(\eta) &= (\alpha_0-\theta)\eta_0^{10} + \alpha_{01}\eta_0^6\eta_1^4 + (\alpha_1-\theta)\eta_1^{10} - \alpha_{02}\eta_0^8\eta_2^2 - \alpha_{12}\eta_1^4\eta_2^6 + (\alpha_2-\theta)\eta_2^{10}.
\end{aligned}
\tag{4.11}
$$

Likewise, for $\{W_i\}$ we get

$$
\begin{aligned}
\widetilde{W}_1(\eta) &= (\beta_1-\theta)\eta_0^8 - \beta_2\eta_0^4\eta_1^4 + \beta_3\eta_0^2\eta_1^6 + (\beta_4-\theta)\eta_1^8 + \beta_5\eta_0^6\eta_2^2\\
&\quad - \beta_6\eta_0^2\eta_1^4\eta_2^2 - \beta_7\eta_1^6\eta_2^2 - \beta_8\eta_1^4\eta_2^4 - \beta_9\eta_0^2\eta_2^6 + (\beta_{10}^+-\theta)\eta_2^8,\\
\widetilde{W}_2(\eta) &= (\beta_1-\theta)\eta_0^8 - \beta_2\eta_0^4\eta_1^4 + \beta_3\eta_0^2\eta_1^6 + (\beta_4-\theta)\eta_1^8 - \beta_5\eta_0^6\eta_2^2\\
&\quad + \beta_6\eta_0^2\eta_1^4\eta_2^2 + \beta_7\eta_1^6\eta_2^2 - \beta_8\eta_1^4\eta_2^4 + \beta_9\eta_0^2\eta_2^6 + (\beta_{10}^--\theta)\eta_2^8,\\
\widetilde{W}_3(\eta) &= (\beta_1-\theta)\eta_0^8 + \beta_2\eta_0^4\eta_1^4 - \beta_3\eta_0^2\eta_1^6 + (\beta_4-\theta)\eta_1^8 + \beta_5\eta_0^6\eta_2^2\\
&\quad + \beta_6\eta_0^2\eta_1^4\eta_2^2 + \beta_7\eta_1^6\eta_2^2 + \beta_8\eta_1^4\eta_2^4 - \beta_9\eta_0^2\eta_2^6 + (\beta_{10}^+-\theta)\eta_2^8,\\
\widetilde{W}_4(\eta) &= (\beta_1-\theta)\eta_0^8 + \beta_2\eta_0^4\eta_1^4 - \beta_3\eta_0^2\eta_1^6 + (\beta_4-\theta)\eta_1^8 - \beta_5\eta_0^6\eta_2^2\\
&\quad - \beta_6\eta_0^2\eta_1^4\eta_2^2 - \beta_7\eta_1^6\eta_2^2 + \beta_8\eta_1^4\eta_2^4 + \beta_9\eta_0^2\eta_2^6 + (\beta_{10}^--\theta)\eta_2^8.
\end{aligned}
\tag{4.12}
$$

Once the forms (4.11) and (4.12) have been determined, the remaining task consists in finding a set of coefficients α which guarantee $\left\{\widetilde{V}_i\right\}$ and $\left\{\widetilde{W}_i\right\}$ to be SOSs and, therefore, PD. This can be approached in a straightforward manner with the aid of a specialized software such as SOSTOOLS (Prajna et al., 2002). This software allows to formulate a SOS problem by defining a set of inequalities as well as the unknowns acting as the decision variables to be found. Thus, recalling the suboptimal gains sets from the previous chapter and substituting their values into the corresponding terms β in (4.8), the coefficients α remain to be the only unknowns to be found. Accordingly, considering the inequalities $\left\{\widetilde{V}_i(\eta) > 0\right\}$ and $\left\{\widetilde{W}_i(\eta) > 0\right\}$, and setting α as the decision variables, a SOS problem can be formulated, from which SOSTOOLS returns the parameters α which render (4.11) and (4.12) SOSs, and consequently, PD; the positive definiteness of (4.2) and (4.7) follows, as a result.

Considering $\theta = 0.1$, the computed LF coefficients α for each of the suboptimal gains sets from Table 3.4 are presented in Table (4.1). As a result, Lyapunov stability is proved; moreover, due to the homogeneity properties of the 2-RED, finite-time global asymptotical stability is ensured for the ideal case without delay.

Set	k_0	k_1	k_2	α_0	α_{01}	α_1	α_{02}	α_{12}	α_2
I	4.55	5.0	1.01	615.5	456	125.9	66.9	31.5	5.8
II	4.5	5.0	0.2	52	34.8	10.4	12.7	13.6	12.3
III	4.83	5.65	1.1	809.8	578.6	149.2	86.7	33.3	5.7
IV	4.84	5.75	0.5	154.6	106.6	29.01	27.8	17.1	6.3
V	5.27	6.87	0.02	70.4	39.7	8.78	19.3	9.2	71.1

Table 4.1: Parameters α for the suboptimal gains sets k miniminizing $|z_1|$.

Note that these results are only known to be valid for the nominal case error dynamics (2.6) with

$\psi = 0$. Therefore, to investigate the robustness in the presence of disturbances, that is, for input signals with $f_0^{(3)}(t) \neq 0$ a further study must be done.

4.2 Stability Analysis for the Perturbed Case

Regarding the perturbed case with $\psi(t) \neq 0$, a maximum bound Δ_0 can be found such that for any disturbance satisfying $|\psi(t)| \leq \Delta_0$, the form W given by (4.7) remains PD and, consequently, the results from the previous section remain valid. Then, considering the coefficients β involving such disturbance in (4.8), the term $\pm\Delta_0$ can be substituted for $\psi(t)$ accounting for its possible extreme values. Accordingly, two different cases can be distinguished:

- the first one, considering Δ_0, with

$$\begin{aligned} \beta_1 &= \frac{5}{3}\alpha_0 k_0 - \alpha_{01} k_1 + \alpha_{02}\left(k_2 + \Delta_0\right), & \beta_{10}^{+} &= \alpha_{12} + 5\alpha_2\left(k_2 + \Delta_0\right), \\ \beta_8 &= 3\alpha_{12}\left(k_2 + \Delta_0\right), & \beta_{10}^{-} &= \alpha_{12} - 5\alpha_2\left(k_2 + \Delta_0\right), \end{aligned} \tag{4.13}$$

- and the second one, considering $-\Delta_0$, with

$$\begin{aligned} \beta_1 &= \frac{5}{3}\alpha_0 k_0 - \alpha_{01} k_1 + \alpha_{02}\left(k_2 - \Delta_0\right), & \beta_{10}^{+} &= \alpha_{12} + 5\alpha_2\left(k_2 - \Delta_0\right), \\ \beta_8 &= 3\alpha_{12}\left(k_2 - \Delta_0\right), & \beta_{10}^{-} &= \alpha_{12} - 5\alpha_2\left(k_2 - \Delta_0\right). \end{aligned} \tag{4.14}$$

Keeping the remaining coefficients of β as defined previously, and substituting the found values of the coefficients α, a new SOS problem can be formulated for each gain set with Δ_0 being the corresponding decision variable. Therefore, the SOSTOOLS software can be used to search for a solution satisfying simultaneously both cases corresponding to Δ_0 and $-\Delta_0$ as given in (4.13) and (4.14), respectively. Such solution will ensure the positive definiteness of the forms $\left\{\widetilde{W}_i\right\}$, and, therefore of W, proving the robustness to bounded disturbances complying with the aforementioned condition $|\psi(t)| \leq \Delta_0$. The determined bounds Δ_0 are shown in Table 4.2, complementing the results from Table (4.1) for the perturbed case.

Set	k_0	k_1	k_2	α_0	α_{01}	α_1	α_{02}	α_{12}	α_2	Δ_0
I	4.55	5.0	1.01	615.5	456	125.9	66.9	31.5	5.8	0.032
II	4.5	5.0	0.2	52	34.8	10.4	12.7	13.6	12.3	0.018
III	4.83	5.65	1.1	809.8	578.6	149.2	86.7	33.3	5.7	0.035
IV	4.84	5.75	0.5	154.6	106.6	29.01	27.8	17.1	6.3	0.027
V	5.27	6.87	0.02	70.4	39.7	8.78	19.3	9.2	71.1	0.002

Table 4.2: Parameters α and Δ_0 for the suboptimal gains sets k minimizing $|z_1|$.

In addition, Δ_0 can be used to provide a scaling for both the gains and the LF coefficients α preserving the stability properties for the perturbed case with bounded disturbances $|\psi(t)| \leq \Delta$ and, consequently, extending the results obtained for the nominal case allowing a broader class of input signals.

According to Sanchez et al. (2016), given a set of coefficients α and gains k such that (4.2) is a LF for the perturbed 2-RED error dynamics (2.6) with a bounded perturbance $\psi(t)$ complying with

$|\psi(t)| \leq \Delta_0$, and considering $|\psi(t)| \leq \Delta$, $\forall t \geq 0$ for any Δ, the origin of (2.6) is finite-time stable with the scaled parameters

$$\bar{k} = \begin{bmatrix} \bar{k}_0 & \bar{k}_1 & \bar{k}_2 \end{bmatrix}^\top = \begin{bmatrix} L^{\frac{1}{3}} k_0 & L^{\frac{2}{3}} k_1 & L k_2 \end{bmatrix}^\top \tag{4.15}$$

where $L = \Delta/\Delta_0$. Moreover, (4.2) is a LF for (2.6) with the scaled coefficients

$$\bar{\alpha} = \begin{bmatrix} \bar{\alpha}_0 & \bar{\alpha}_{01} & \bar{\alpha}_1 & \bar{\alpha}_{02} & \bar{\alpha}_{12} & \bar{\alpha}_2 \end{bmatrix}^\top = \begin{bmatrix} L^{-\frac{5}{3}} \alpha_0 & L^{-2} \alpha_{01} & L^{-\frac{5}{2}} \alpha_1 & L^{-\frac{7}{3}} \alpha_{02} & L^{-4} \alpha_{12} & L^{-5} \alpha_2 \end{bmatrix}^\top. \tag{4.16}$$

Although such results assume noiseless continuous-time conditions, the scaling can still be used for the considered case under a time delay to guarantee bounded trajectories for an input base signal $f_0(t)$ satisfying $\left| f_0^{(3)}(t) \right| \leq \Delta$.

4.3 Numeric Example

In order to illustrate the scaling procedure, consider an input signal $f(t) = \cos(2t)$ for which the considered suboptimal gains of set I from Table 4.2 cannot longer deal with the corresponding disturbance $|\psi| \leq 8$. Thus, for the corresponding bounds $\Delta_0 = 0.032$ and $\Delta = 8$ a scaling term $L = 250$ is obtained. Applying such scaling, the simulation results for the differentiation error ε_1 are shown in Figs. (4.1) and (4.2) for both cases with and without considering the Padé approximation; additionally, the case for a scaling term $L = 10$ is also plotted. It can be noticed that although both scalings allow the differentiator to converge to a permanent state oscillatory regime, that with $L = 250$ gives rise to a considerably greater *chattering* amplitude in comparison with the other selected scaling term which despite being two orders of magnitude smaller, allows to deal with the disturbance too. This fact may be explained due to the conservative bound Δ_0 found previously that leads to an overestimation of the corresponding scaling L. Therefore, although the mentioned procedure works, it would be more convenient to choose a smaller scaling gain by other means in order to improve the steady-state performance.

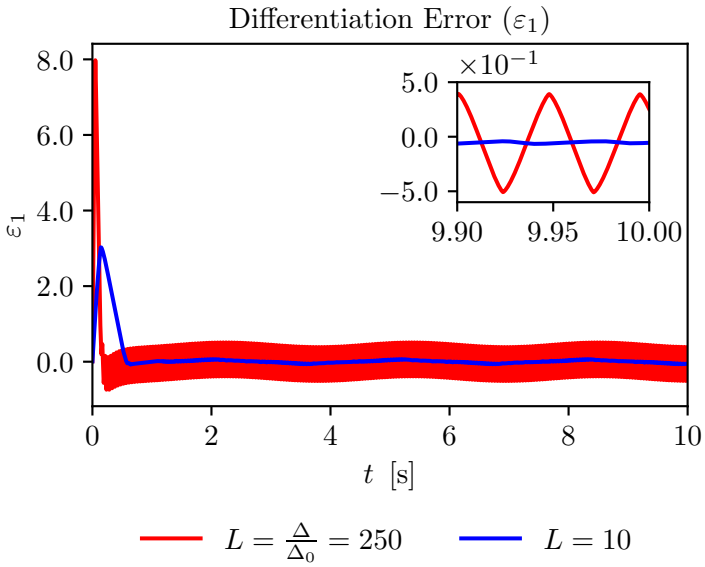

Figure 4.1: Simulation results for ε_1 considering a delay $\mu = 0.01$ and the suboptimal gains of set I from Table 4.2. $f(t) = \cos(2t)$ is considered as input signal.

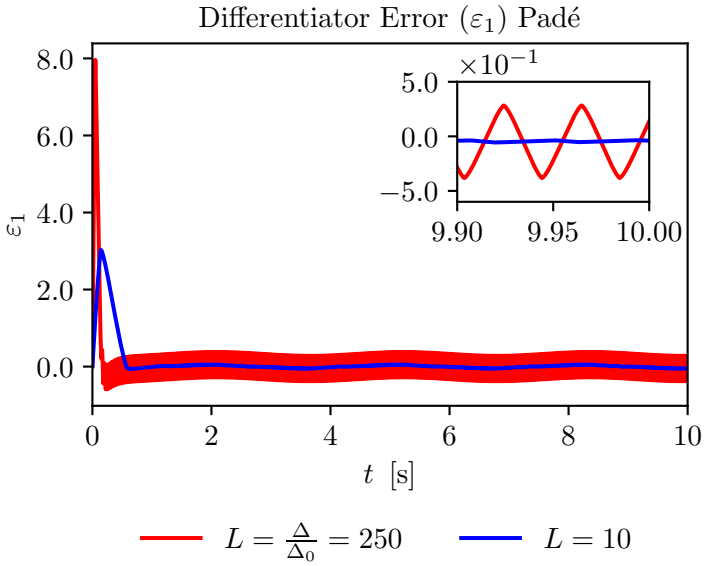

Figure 4.2: Simulation results for ε_1 considering a delay $\mu = 0.01$ using a Padé approximation and the suboptimal gains of set I from Table 4.2. $f(t) = \cos(2t)$ is considered as input signal.

Chapter 5

Conclusions

During this work, the issue of the gains design for the 2-RED was studied under a frequency approach. Taking advantage of the structure of the differentiator, a DF for such system was computed under the assumption that a constant time delay may account for the nonidealities giving rise to the *chattering* phenomenon during a real-time differentiation task. Furthermore, considering that the resulting motion could be decomposed as arising from two different subsystems, one pertaining to a slow component, and the other related to comparatively fast steady-state self oscillations, the DF method was used to investigate the permanent regime oscillatory response. Based on such technique and considering a first order approximation for the delay, a selection criterion for the parameters of the differentiator was found meeting the stated objectives of this work. Namely,

- approximated amplitude values for the possible oscillations due to the introduction of the time delay were calculated as a function of the differentiator gains,
- some suboptimal sets of gains leading to a minimization of the computed oscillations amplitude were found,
- it was shown that if the expected oscillations exist, they are to be orbitally asymptotically stable,
- moreover, it was proved that the ideal differentiator without delay preserves global finite time convergence given such suboptimal sets of parameters.

Additionally, the extension of such results to the perturbed case was suggested by considering a scaling given as a function of estimated upper bounds of the allowed disturbances for the nominal case.

With respect to the practical usefulness of these results, comparison between the steady-state estimated performance of the suboptimal gains via the frequency methods and that determined via simulations show a close agreement if the assumption of a first order Padé approximant for the delay holds; the likeness of the expected behavior is not quite as exact when such approximation is dismissed, though. This could be further explained due to the fact that the DF is an approximation technique too. Therefore, this approach may result better-suited for a qualitative study as exemplified in the present work. Although the predicted *chattering* amplitude may not match accurately the actual one arisen in the simulations, restricting the attention to the latter, the amplitude values corresponding to the determined suboptimal gains do not differ too much from

the actual minima. As such, the devised selection criterion could be regarded as an assisting, yet not so straightforward to use, tool to enhance the performance of given parameters sets since it involves the numerical solution of some equations. Moreover, a further study needs to be done in order to reliably assert for which kind of input signals such results remain valid as well as assess their consistency under the presence of measurement noise. Finally, their congruence with existent results concerning discretization could be investigated too.

In view of the aforementioned issues, future work aiming to improve the reliability of the results yielded by the gains selection criterion could be encompassed in two different directions: the first one regarding the considered model of the time delay and the second one pertaining the frequency method to be used. With respect to the time delay, a higher-order approximation may be introduced, or even it could be attempted to exclude such approximation. Concerning the frequency method to be used, some more complex techniques known to render more accurate results such as the DIDF, the LPRS and that due to Tsypkin may be studied. Moreover, both research lines could be merged.

References

Andrieu, V., Praly, L., & Astolfi, A. (2008). Homogeneous approximation, recursive observer design, and output feedback. *SIAM Journal on Control and Optimization*, *47*(4), 1814–1850.

Atherton, D. P. (1996). Early developments in nonlinear control. *IEEE Control Systems Magazine*, *16*(3), 34–43.

Baker, G. A., Baker Jr, G. A., Graves-Morris, P., Baker, G., & Baker, S. S. (1996). *Pade approximants: Encyclopedia of mathematics and it's applications, vol. 59 george a. baker, jr., peter graves-morris* (Vol. 59). Cambridge University Press.

Barbot, J.-P., Levant, A., Livne, M., & Lunz, D. (2020). Discrete differentiators based on sliding modes. *Automatica*, *112*, 108633.

Beals, R., & Wong, R. (2010). *Special functions: A graduate text* (Vol. 126). Cambridge University Press.

Bernuau, E., Efimov, D., Perruquetti, W., & Polyakov, A. (2013). On an extension of homogeneity notion for differential inclusions. *2013 European Control Conference (ECC)*, 2204–2209.

Bernuau, E., Efimov, D., Perruquetti, W., & Polyakov, A. (2014). On homogeneity and its application in sliding mode control. *Journal of the Franklin Institute*, *351*(4), 1866–1901.

Bhat, S. P., & Bernstein, D. S. (1997). Finite-time stability of homogeneous systems. *Proceedings of the 1997 American control conference*, *4*, 2513–2514.

Boiko, I. (2003). Frequency domain analysis of fast and slow motions in sliding modes. *Asian Journal of Control*, *5*(4), 445–453.

Boiko, I. (2005). Analysis of sliding modes in the frequency domain. *International Journal of Control*, *78*(13), 969–981.

Boiko, I. (2018). On Loeb's criterion of orbital stability of self-excited periodic motions. *2018 15th International Workshop on Variable Structure Systems (VSS)*, 464–469.

Boiko, I., Castellanos, I., & Fridman, L. (2008). Analysis of response of second-order sliding mode controllers to external inputs in frequency domain. *International Journal of Robust and Nonlinear Control: IFAC-Affiliated Journal*, *18*(4-5), 502–514.

Boiko, I., Fridman, L., Pisano, A., & Usai, E. (2007). Analysis of chattering in systems with second-order sliding modes. *IEEE transactions on Automatic control*, *52*(11), 2085–2102.

Chalanga, A., Kamal, S., Fridman, L. M., Bandyopadhyay, B., & Moreno, J. A. (2016). Implementation of super-twisting control: Super-twisting and higher order sliding-mode observer-based approaches. *IEEE Transactions on Industrial Electronics*, *63*(6), 3677–3685.

Cruz-Zavala, E., & Moreno, J. A. (2018). Levant's arbitrary-order exact differentiator: A Lyapunov approach. *IEEE Transactions on Automatic Control*, *64*(7), 3034–3039.

Cruz-Zavala, E., Moreno, J. A., & Fridman, L. M. (2011). Uniform robust exact differentiator. *IEEE Transactions on Automatic Control*, *56*(11), 2727–2733.

Dabroom, A., & Khalil, H. K. (1997). Numerical differentiation using high-gain observers. *Proceedings of the 36th IEEE Conference on Decision and Control*, *5*, 4790–4795.

Filippov, A. F. (1988). *Differential equations with discontinuous righthand sides*. Kluwer Academic Publishers.

Fossard, A., & Floquet, T. (2002). Introduction: An overview of classical sliding mode control. In W. Perruquetti & J.-P. Barbot (Eds.), *Sliding mode control in engineering*. Marcel Dekker.

Fridman, L., Moreno, J. A., Bandyopadhyay, B., Kamal, S., & Chalanga, A. (2015). Continuous nested algorithms: The fifth generation of sliding mode controllers. In X. Yu & M. Önder Efe (Eds.), *Recent advances in sliding modes: From control to intelligent mechatronics* (pp. 5–35). Springer.

Gelb, A., & Vander Velde, W. E. (1968). *Multiple-input describing functions and nonlinear system design*. McGraw Hill.

Hardy, G. H., Littlewood, J., & Pólya, G. (1988). *Inequalities* (2nd ed.). Cambridge University Press.

Hermes, H. (1991). Homogeneous coordinates and continuous asymptotically stabilizing feedback controls. In S. Elaydi (Ed.), *Differential equations: Stability and control* (pp. 249–260). Marcel Dekker.

Hung, J. Y., Gao, W., & Hung, J. C. (1993). Variable structure control: A survey. *IEEE transactions on industrial electronics*, *40*(1), 2–22.

Kalman, R. E. (1960). A new approach to linear filtering and prediction problems.

Khalil, H. K. (2002). *Nonlinear systems* (3rd ed.). Prentice Hall.

Lang, S. (2002). *Algebra*. Springer.

Levant, A. (1998). Robust exact differentiation via sliding mode technique. *automatica*, *34*(3), 379–384.

Levant, A. (2003). Higher-order sliding modes, differentiation and output-feedback control. *International journal of Control*, *76*(9-10), 924–941.

Levant, A. (2010). Chattering analysis. *IEEE transactions on automatic control*, *55*(6), 1380–1389.

Levant, A., & Livne, M. (2020). Robust exact filtering differentiators. *European Journal of Control*, *55*, 33–44.

Livne, M., & Levant, A. (2014). Proper discretization of homogeneous differentiators. *Automatica*, *50*(8), 2007–2014.

Mboup, M., Join, C., & Fliess, M. (2009). Numerical differentiation with annihilators in noisy environment. *Numerical algorithms*, *50*(4), 439–467.

Merino, M. F. (2019). *Cálculo recursivo de ganancias para el diferenciador de levant por medio de funciones de lyapunov* (MEng thesis).

Moreno, J. A. (2012). Lyapunov function for levant's second order differentiator. *2012 IEEE 51st IEEE conference on decision and control (CDC)*, 6448–6453.

Moreno, J. A. (2018). Exact differentiator with varying gains. *International Journal of Control*, *91*(9), 1983–1993.

Obeid, H., Fridman, L., Laghrouche, S., Harmouche, M., & Golkani, M. A. (2018). Adaptation of Levant's differentiator based on barrier function. *International Journal of Control*, *91*(9), 2019–2027.

Ortiz-Ricardez, F. A., Sánchez, T., & Moreno, J. A. (2015). Smooth Lyapunov function and gain design for a second order differentiator. *2015 54th IEEE Conference on Decision and Control (CDC)*, 5402–5407.

Papachristodoulou, A., & Prajna, S. (2002). On the construction of Lyapunov functions using the sum of squares dfecomposition. *Proceedings of the 41st IEEE Conference on Decision and Control, 2002.*, *3*, 3482–3487.

Parrilo, P. A. (2000). *Structured semidefinite programs and semialgebraic geometry methods in robustness and optimization* (PhD thesis).

Pérez-Ventura, U., & Fridman, L. (2019a). Design of super-twisting control gains: A describing function based methodology. *Automatica*, *99*, 175–180.

Pérez-Ventura, U., & Fridman, L. (2019b). When is it reasonable to implement the discontinuous sliding-mode controllers instead of the continuous ones? frequency domain criteria. *International Journal of Robust and Nonlinear Control*, *29*(3), 810–828.

Pérez-Ventura, U., Mendoza-Avila, J., & Fridman, L. (2021). Design of a proportional integral derivative-like continuous sliding mode controller. *International Journal of Robust and Nonlinear Control*.

Perruquetti, W., Floquet, T., & Moulay, E. (2008). Finite-time observers: Application to secure communication. *IEEE Transactions on Automatic Control*, *53*(1), 356–360.

Prajna, S., Papachristodoulou, A., & Parrilo, P. A. (2002). Introducing SOSTOOLS: A general purpose sum of squares programming solver. *Proceedings of the 41st IEEE Conference on Decision and Control, 2002.*, *1*, 741–746.

Rabiner, L., & Steiglitz, K. (1970). The design of wide-band recursive and nonrecursive digital differentiators. *IEEE Transactions on Audio and Electroacoustics*, *18*(2), 204–209.

Reichhartinger, M., & Spurgeon, S. (2018). An arbitrary-order differentiator design paradigm with adaptive gains. *International Journal of Control*, *91*(9), 2028–2042.

Sanchez, T., Cruz-Zavala, E., & Moreno, J. A. (2018). An SOS method for the design of continuous and discontinuous differentiators. *International Journal of Control*, *91*(11), 2597–2614.

Sanchez, T., & Moreno, J. A. (2019). Design of Lyapunov functions for a class of homogeneous systems: Generalized forms approach. *International Journal of Robust and Nonlinear Control*, *29*(3), 661–681.

Sanchez, T., Moreno, J. A., & Fridman, L. M. (2018). Output feedback continuous twisting algorithm. *Automatica*, *96*, 298–305.

Sanchez, T., Moreno, J. A., & Ortiz-Ricardez, F. A. (2016). Construction of a smooth Lyapunov function for the robust and exact second-order differentiator. *Mathematical Problems in Engineering*, *2016*.

Shtessel, Y., Edwards, C., Fridman, L., Levant, A., et al. (2014). *Sliding mode control and observation* (Vol. 10). Springer.

Slotine, J.-J. E., & Li, W. (1991). *Applied nonlinear control*. Prentice Hall.

Utkin, V., & Lee, H. (2006). The chattering analysis. *2006 12th International Power Electronics and Motion Control Conference*, 2014–2019.

Utkin, V., Poznyak, A., Orlov, Y., & Polyakov, A. (2020). Conventional and high order sliding mode control. *Journal of the Franklin Institute*, *357*(15), 10244–10261.

Zubov, V. I. (1964). *Methods of A.M. Lyapunov and their application*. P. Noordhoff.